Heavy Truck Modeling for Fuel Consumption
Simulations and Measurements

Tony Sandberg

Division of Vehicular Systems
Department of Electrical Engineering
Linköping University, S–581 83 Linköping, Sweden
http://www.vehicular.isy.liu.se/
Email: tony@isy.liu.se

Linköping 2001

**Heavy Truck Modeling for Fuel Consumption
Simulations and Measurements**

*Department of Electrical Engineering,
Linköping University,
S–581 83 Linköping,
Sweden.*

To Pernilla, Pontus and Anton

Abstract

Fuel consumption for heavy trucks depends on many factors like roads, weather, and driver behavior that are hard for a manufacturer to influence. However, one design possibility is the powertrain configuration. Here a new simulation program for heavy trucks is created to find the configuration of the powertrain that gives the lowest fuel consumption for each transport task.

For efficient simulations the model uses production code for speed and gear control, and it uses exchangeable data sets to allow simulation of the whole production range of engine types, on recorded road profiles from all over the world. Combined with a graphical user interface this application is called STARS (Scania Truck And Road Simulation).

The forces of rolling resistance and air resistance in the model are validated through an experiment where the propeller shaft torque of a heavy truck is measured. It is found that the coefficient of rolling resistance is strongly dependent on tire temperature, not only on vehicle speed as expected. This led to the development of a new model for rolling resistance. The model includes the dynamic behavior of the tires and relates rolling resistance to tire temperature and vehicle speed.

In another experiment the fuel consumption of a test truck in highway driving is measured. The altitude of the road is recorded with a barometer and used in the corresponding simulations. Despite of the limited accuracy of this equipment the simulation program manage to predict a level of fuel consumption only 2% lower than the real measurements.

It is concluded that STARS is a good tool for predicting fuel consumption for trucks in highway driving and for comparing different powertrain configurations.

Acknowledgment

This work has been carried out between April 1999 and December 2001 at Vehicular Systems, Linköping University and Scania CV AB in Södertälje.

I would like to express my gratitude to a number of people:

My Professor Lars Nielsen for the supervision and the many interesting discussions. The staff at Vehicular Systems for creating a positive atmosphere. Especially Erik Frisk and Lars Eriksson for giving me feedback on drafts of this manuscript.

My managers, Per-Ola Post and Peter Wansölin at the department of Engine Development at Scania for believing in me and for giving me this opportunity. Håkan Fransson for giving me the inspiration. All others at Scania who helped me with test equipment and inspiring discussions.

Finally, I would like to thank my family. My wife, Pernilla, for being there and supporting me, our sons, Pontus and Anton for all the happiness and pride you bring into our lifes.

<div style="text-align: right;">

Södertälje, December 2001
Tony Sandberg

</div>

8

Contents

10

1

Introduction

Trucks are sold in another way compared to passenger cars. The customer can choose his own combination of parts, including type of engine, gearbox, central gear etc. The selection is based on the customers transport task and previous experiences. To reduce fuel consumption it is important to choose a powertrain combination (gearbox, central gear ratio, tire dimension) that allows efficient use of the engine. Such an optimization of powertrain configuration is a complex task, but current simulation techniques provide means to reduce costly testing by replacing it partly with analysis. The goal of this thesis is to investigate models and methods needed for such analysis and optimization.

The core of the problem is to find a model that captures fuel consumption. The requirements on the model are that the characteristic behaviors are captured, that the absolute precision must be satisfactory, and that it is possible to judge relative differences between different powertrain configurations. It turns out that such a model not only requires a basic vehicle model, but also requires several other components like e.g. driver behavior, road descriptions, descriptions of typical missions, engine usage, and behavior of the control systems of the vehicle (like engine control and transmission control).

In this thesis factors for fuel consumption have been considered, modeling has been performed, a tool for vehicle simulation aiming at powertrain evaluation has been developed, and two main types of experiments have been performed to validate the model qualitatively and quantitatively. One type of experiment uses an extra torque sensor on the propeller shaft to validate the major energy losses, like air resistance and rolling resistance, on designed test range experiments. The other main type of experiment has been comparing

13

measurements and simulations of fuel consumption for a heavy truck in usual highway driving. The overall results are indicated in the thesis outline following below.

1.1   Outline and Contributions

Chapter 2 contains an introductory background. It explains the importance of low fuel consumption, which factors that influence it most, and discuss the difficulty of measuring it accurately in real trucks. Finally, the advantages and needs for a simulation program to study fuel consumption is discussed.

In Chapter 3 a physical longitudinal vehicle model of a heavy truck in motion on a longitudinal road is presented. The aim is to capture the essential parts for fuel consumption in the model.

The first main result of the thesis is presented in Chapter 4. It is a program built to simulate fuel consumption for trucks in highway driving, called STARS (Scania Truck And Road Simulation). The primary use of the program is to study the influence of different powertrain configurations on fuel consumption. Examples of user requirements and design requirements are modular design, exchangeable data sets and the use of production code within the model. The model is implemented in the modeling language Modelica using the software Dymola. The chapter ends with a presentation of the graphical user interface, built in Matlab, to control the vehicle model.

Chapter 5 and Chapter 6 deal with the results and interpretation of designed test track experiments to validate energy losses like rolling resistance and air resistance. Experiments are performed by driving a vehicle at constant speed on a road with constant slope while measuring torque on the propeller shaft together with vehicle speed. Tests at different speeds are used to identify forces of rolling resistance and air resistance. The model is adjusted to agree with the measurements. One important observation here is the unexpected dynamic behavior of the tires. It is found that the coefficient of rolling resistance is strongly dependent on tire temperature and not only on vehicle speed as expected. This led to another main contribution of this work, the new model for rolling resistance presented in Chapter 6. This model includes the dynamic behavior of the tires and relates rolling resistance to tire temperature and vehicle speed.

Experiments to validate fuel consumption under usual driving conditions are presented in Chapter 7. This means that the the whole model is considered, not only the parts validated in the previous chapters. A heavy truck is driven on a highway and fuel consumption is measured. As mentioned above, these measurements are not easy to perform, so a sensitivity analysis is conducted, and important parameters are pointed out. Validation is performed by comparing measurements and simulations of fuel consumption. The results show that STARS is a sufficient platform to predict fuel consumption for trucks in highway driving, and further that it is well suited to perform comparisons between powertrain configurations.

2

Fuel Consumption

Fuel consumption has been a core consideration since the beginning of the transportation era. The are reasons related to our environment, and to economics. In the competitive truck industry fuel consumption is an important sales argument, since customers on average drive their trucks distances of 150 000 km per year, which means that fuel becomes a large part of the lifetime cost for a vehicle.

   In the first section below, major causes of fuel consumption are described. It is also explained which of those the truck manufacturer can influence. One possibility, namely powertrain configuration is presented in Section 2.2. The two last sections deal with the difficulties of doing reliable measurements of fuel consumption and a discussion of the need for a simulation program.

2.1 Influencing Factors

Fuel consumption depends on a lot of factors; speed and weight of the vehicle are the most important because they effect the rolling resistance, air resistance and the resistance due to inclination of the road. This is illustrated in Figure 2.1 showing how the energy produced by the engine is divided into different energy losses. Data is generated with a simulation of a 40 ton truck on a typical road. Only points were the engine produces power are taken into account (no downhills). Due to the large weight, the largest loss is in potential energy when climbing up hills. About 30% of the energy is lost as rolling resistance in the tires and 23% is lost as air resistance. The rest, around 7%, comes from losses in wheel bearings, the central gear, the gearbox, and engine auxiliary units.
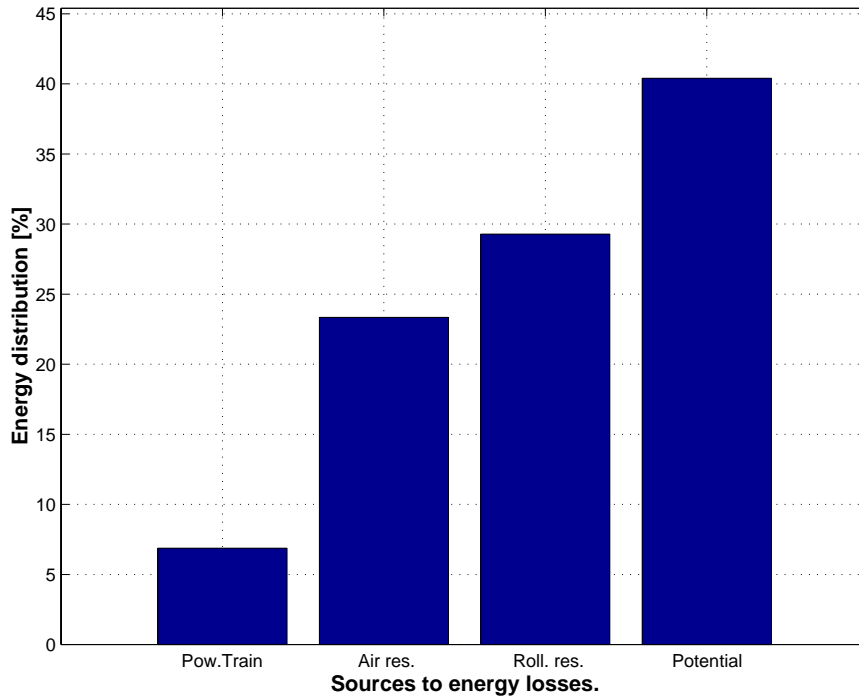
Figure 2.1: A simulation of a 40 ton truck on a typical road shows that most of the energy produced by the engine is used to climb the hills.

From the truck manufacturer's point of view the basic factors speed and weight are hard to influence. The speed is determined by the driver, and the weight of the vehicle by how much cargo it is transporting. Reducing the empty weight of the truck is of course important, but in many cases it primarily leads to more payload, not less total weight. The existing road profile has to be accepted even though we might wish for flat roads. Low rolling resistance has a high priority when tire manufacturers develop new tires. When it comes to air resistance, truck manufacturers can only work with the front end, the cabin, to make aerodynamic adjustments. The rear end of trucks is usually box shaped to enable as much cargo as possible and it is also designed by others. At this point, after many years of cab development, further big reductions of the aerodynamic resistance are hard to achieve. On the last part in Figure 2.1, the energy losses in the powertrain, much work is spent to find better control of the auxiliary units but it is hard to find more efficient design of the gears.

This section has shown that it is hard for the truck manufacturer to reduce fuel consumption much through traditional methods. Therefore other parts of the vehicle, such as the powertrain configuration becomes more important.

2.2 Powertrain Configuration

When buying a truck, the customer can choose his own combination of parts, including type of engine, gearbox, cabin etc. This selection is then based on the customers transport task and previous experiences.

However, depending on the aim, lowest fuel consumption, lowest price, maximum payload, best comfort etc, there exists many optimal combinations of parts. To reduce fuel consumption it is important to utilize the engine as efficiently as possible. This means to choose a tire dimension, central gear ratio and gearbox that allows the engine to operate in a good operational point for as much time of the transport task as possible. A good operational point is the combination of engine speed and load where the specific fuel consumption of the engine is low. The procedure of choosing good combinations of engine, gearbox, central gear ratio and tire dimension is called powertrain configuration.

The potential of powertrain configuration is shown in Figure 2.2 where the same simulation as in Figure 2.1 is illustrated but here the base is the amount of energy put in to the engine through the fuel. As seen, almost 60% of this energy is transformed to heat in the engine which is the totally dominating loss of energy. By tailoring the powertrain configuration for each type of transport, the efficiency of engine over the whole distance can be increased, losses like in Figure 2.2 and fuel consumption can be reduced.

If only studying fuel consumption, one solution could be to choose a small and weak engine to achieve a low fuel consumption. However, this vehicle would require numerous gearshifts to manage the transport task. This situation is an example of poor driveability. It would be very tiresome to drive this vehicle and the owner could eventually have problems to find drivers willing to work in the vehicle.

Therefore, it is important for a manufacturer to make recommendations to the customer of which powertrain combination to buy, depending on the transport task. The recommendation must take both fuel consumption and driveability into account.

2.3 Difficulties with Measurements

Doing reliable measurements of fuel consumption in a real vehicle is complicated and time consuming. The main problem is that surrounding factors are not repeatable. While the vehicle is being rebuilt to another configuration, surrounding factors like weather and traffic-load change. An alternative is to use several vehicles at the same time (at considerable cost), but still there are unwanted differences between the individual vehicles and drivers. How hard the driver accelerates and at which engine speeds gears are changed can influence fuel consumption by 5%. Additionally, the differences between different vehicle configurations are usually very small, so it is necessary to drive long distances to ensure a certain difference.
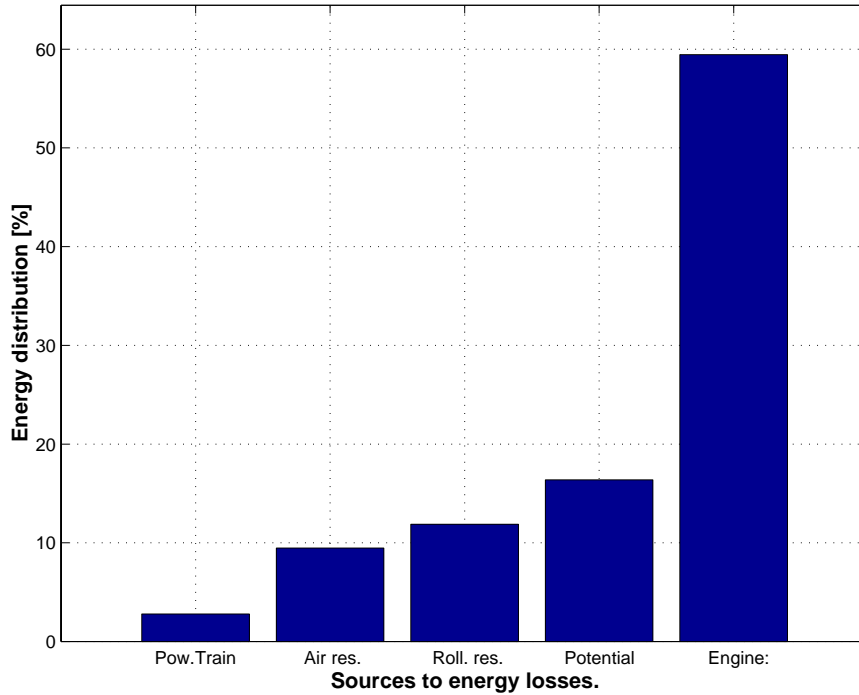
Figure 2.2: Distribution of the energy put in to (in the fuel) the engine for a 40 ton truck simulated on a typical road. Since the efficiency of the engine is about 40% there is a large potential to improve this.

2.4   The Need for a Simulation Program

It is obvious from the previous discussion that there are considerable advantages, e.g. for Scania, with a simulation program to perform studies of fuel consumption with emphasis on powertrain configuration. By use of computer simulations a repeatable result of fuel consumption can be created and differences between vehicles can be studied. The simulation program needs a vehicle model to be able to simulate a truck in many hours of highway driving. These simulations should be used for statistics, comparisons of fuel consumption, emissions and average speeds. To facilitate simulations of long driving distances with short calculation times the vehicle model needs to be rather computationally efficient. In order to optimize the configuration of the powertrain it shall be possible to simulate the whole production range of engines, gearboxes, central gears, tire treads and dimensions.

3

Model

This chapter presents the models created to describe the energy losses that influence fuel consumption, as discussed in Chapter 2. Recall that the requirements on such a model are that the characteristic behaviors are captured, that the absolute precision must be satisfactory, and that it is possible to judge relative differences between different powertrain configurations. These tasks require not only a basic vehicle model, but also several other components like e.g. driver behavior, road descriptions, descriptions of typical missions, engine usage, and behavior of the control systems of the vehicle (like engine control and transmission control).

The overall vehicle model is longitudinal, and Figure 3.1 show its hierarchial structure. Each box symbolise a component. This structure follows the structure of the real vehicle and also the way truck development is organized at Scania. The model components are presented starting with the basic mechanics equations of the vehicle in Section 3.1. Thereafter the engine model is presented in Section 3.2. The engine model is based on steady state values from from engine test-cell experiments. The engine control system is represented by real production code. The powertrain components between the engine and the wheels are described in Section 3.3. The gearbox model and the hydraulic retarder brake are controlled by production code. In Section 3.4 the wheel model is described. Much attention is spent on wheel models since rolling radius and rolling resistance are important parts in this kind of simulation. This problem will be addressed further in Chapter 5 and Chapter 6. The model of the driver is treated in Section 3.5, and Section 3.6 ends the chapter with a description of the surroundings of the vehicle, the road and air conditions.
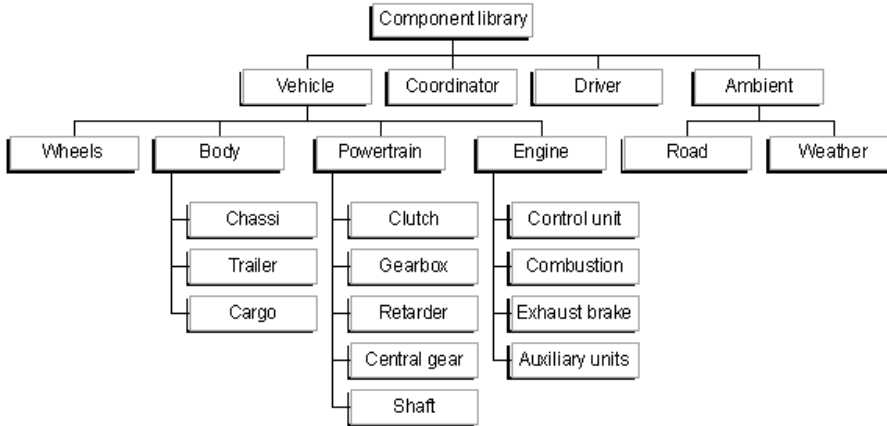
Figure 3.1: Structure of the vehicle model.

3.1   Vehicle Body

The vehicle body is divided into three components; chassis, trailer and cargo. Together they are used to model weight, to distribute it properly to different axles, to symbolize air resistance and represent the inertia in the system. The vehicle model is longitudinal since suspension and steering (cornering) does not have a large influence on fuel consumption.

3.1.1   Chassis

The main part of the vehicle model is the chassis. The position, speed and acceleration of the vehicle are determined through Newton's second law of motion

$$\sum F_i = m \cdot a \tag{3.1}$$

where F_i are all forces acting on the chassis in the longitudinal direction, m is its mass, and a is the longitudinal acceleration of the chassis.

All forces acting on the chassis are shown in Figure 3.2. The dark squares are cuts, interfaces, to other modules. Beside the forces in the x and y direction in every cut (from the wheels and the drawbars), the chassis is affected by the air resistance, R_a, a gravitational force, Mg and a service brake force, BF. The equilibrium equations follows from standard textbooks, like (Kiencke and Nielsen, 2000). With variables defined as in Figure 3.2, and by letting θ denote

Figure 3.2: Forces on longitudinal chassis model.

the slope of the road, this leads to

$$
\begin{aligned}
FB_x + RB_x + D_x + F_x - M \cdot g \cdot \sin\theta - BF - R_a &= M \cdot a \quad &(3.2)\\
FB_y + RB_y + D_y + F_y - M \cdot g \cdot \cos\theta &= 0 \quad &(3.3)
\end{aligned}
$$

$$
\begin{aligned}
M \cdot g \cdot \cos\theta \cdot l_f + (M \cdot g \cdot \sin\theta + BF) \cdot h + \\
R_a \cdot h_a - D_x \cdot h_d - D_y \cdot (l_r + l_d) - \\
F_x \cdot h_5 - F_y \cdot (l_r - l_5) - RB_y \cdot l_r &= 0 \quad (3.4)
\end{aligned}
$$

As illustrated by these equations the chassis has a dynamic weight distribution between front and rear axle.

Air Resistance

The aerodynamic resistance is generated by two sources: one is the airflow around the vehicle body and the other is the flow through the engine radiator system and the interior of the vehicle. Of the two, the former is the dominant one and generates normal pressure and shear stress on the vehicle body. The effect of aerodynamic forces is largest at moderate or higher speed. In (Wong, 1993), the aerodynamic resistance is expressed by

$$
R_a = \frac{\rho}{2} \cdot C_D \cdot A_f \cdot v_r^2 \quad (3.5)
$$

where ρ is the mass density of the air, C_D is the coefficient of aerodynamic resistance, A_f is the characteristic area of the vehicle, usually taken as the

Figure 3.3: Trailer module used to distribute the weight of the vehicle on three different axels.

frontal area, and v_r is the speed of the vehicle relative to the wind. Because it is impossible to know the direction of the wind at all times in reality, the wind speed is neglected in the model using the vehicle speed instead, $v_r = v$. Effects of side wind is partly covered by using special values for C_D. The used value is not only longitudinal but includes some side winds. The frontal area is the projected area of the vehicle in the direction of travel, for trucks this is about 9-12 m^2 (passenger cars have about 2 m^2).

The coefficient of aerodynamic resistance C_D is mainly a function of the shape of the vehicle body. Trucks and busses are usually box shaped since this shape enables most storage space. Typical values of C_D for trucks and buses are 0.5-1.1. Passenger cars usually have values of C_D around 0.3. Aerodynamic lift is neglected due to the boxed shape of trucks.

3.1.2   Trailer

Heavy trucks usually have a trailer or a wagon to carry a major part of the cargo. This makes them longer and gives more place for cargo, but also distribute the weight among more axles and thus minimize the wear on the roads. Including a trailer in the vehicle model enables the correct load on each type of axle, which is advantageous , since different types of tires normally are used on trucks and trailers. Since the coefficient of rolling resistance differs with the type of tire, the correct load on each axle is important when calculating rolling resistance.

The model of the trailer is illustrated in Figure 3.3. It is simply a rigid beam, without own mass, between the truck and the last axle, on which a weight (the cargo) can be placed. The equilibrium equations are simple and are omitted.

3.1.3   Cargo

The cargo module, symbolized in Figure 3.4, is used to model the pay-load and is therefore the second mass (the mass of chassis being the first). It is rigidly connected to the chassis through the trailer. Like all other masses it is affected
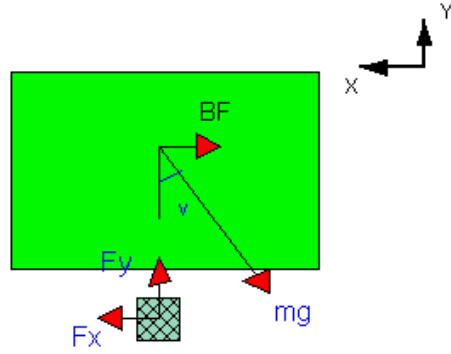
Figure 3.4: Cargo module, can be placed on the chassis or the trailer module.

by gravity, including the effect of the slope of the road. If the trailer is removed from the vehicle model, the cargo can be placed directly on the chassis.

3.2 Engine

In heavy trucks diesel engines are used almost exclusively. The engine size is in the range from 9 to 16 liters and 200 to 600 hp. They are usually turbo charged and equipped with direct fuel injection. The amount of fuel to inject and its timing is commonly calculated by a electronic control unit.

Only parts that affect the motion of the vehicle in the longitudinal direction are modeled in this work. The engine model shown in Figure 3.5 is built up by four submodels: control unit, combustion, exhaust brake and auxiliary units. The model of the control unit determines the amount fuel to the engine by use of production code. The model of the combustion uses steady state maps from engine test-cell to describe the conversion of fuel to torque. The exhaust brake also uses measured values to model how much the engine is braked when it is activated. The auxiliary units represent a constant loss of torque.

3.2.1 Control Unit

The control unit is represented by the actual C-code used in production vehicles to control the amount of fuel injected to the engine. The main part is the cruise control used to control the vehicle speed by comparing the vehicle speed to the reference speed and then calculating the fueling. The amount of fuel from the cruise control is limited by the maximum fueling curve. A principal view of the incremental gain scheduled PID-controller is shown in Figure 3.6. Figure 3.7 shows the response to a step change in reference speed from 70 km/h to 80 km/h executed after 20 seconds. The response time for the system is 15 seconds. The lower part of the figure shows fueling to the engine with a fast and stable
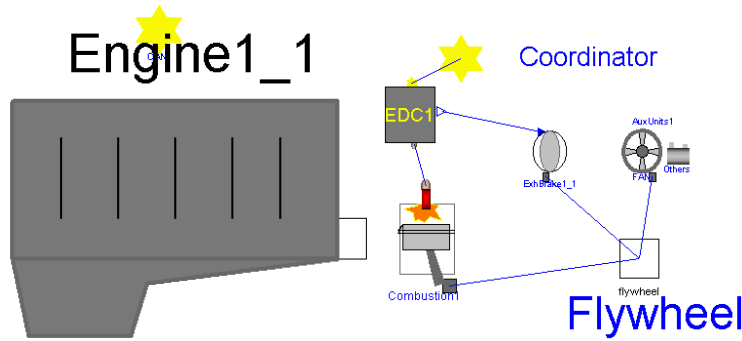
Figure 3.5: Left: top layer (icon) of engine model. Right: submodels that build up the engine model; control unit, combustion, exhaust brake and auxiliary units.
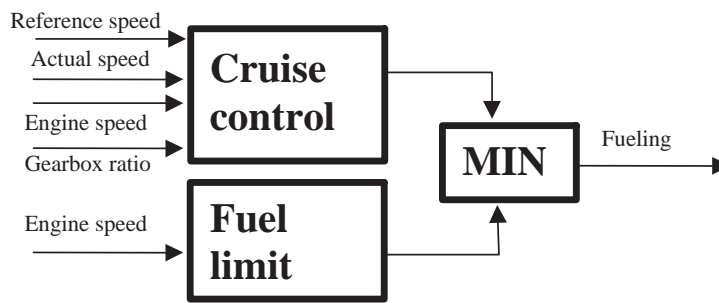
Figure 3.6: Principal view of the controller for cruise control

reaction. The model used is a truck on flat road with total weight of 40 ton, and a 420 hp engine.

The vehicle model is always controlled by the cruise control and the model of the driver can not turn it off. This solution was chosen instead of modeling a gas pedal and a driver who press it more or less depending on the actual speed. With this solution a better speed control can probably be achieved.

3.2.2   Combustion

As will be seen in Chapter 7, the engine operates near steady state conditions during highway driving. Transient operation mainly occurs during take off and gear shifting. For a highway truck this can be considered to happen rarely. Due to these facts, engine operation during highway driving can be described well by using steady state maps from engine test-cell. In these maps, all states like engine speed, torque, boost pressure, temperatures and so on, have reached stable and constant values for all measured operating points. The function of
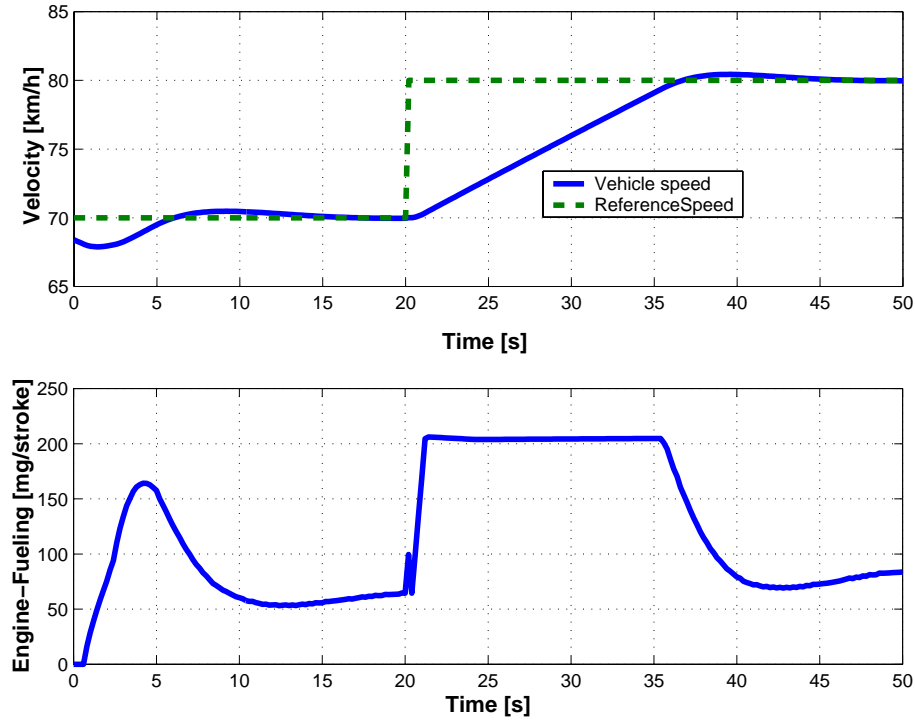
Figure 3.7: Response to step in reference speed, top: vehicle speed and reference speed, bottom: fueling to the engine.

the turbo and the injection system is included in these maps.

The operational area of an engine is described by three curves as in Figure 3.8. Curve A shows the maximum torque the engine can produce. Curve B illustrates idle, when the engine only cope to propel it self. Curve C tells the engine drag, i.e. how much friction torque the engine has when it is driven by an external torque without fuel supply. This approach provides a way to describe the whole engine operational area at the same time. The engine normally operates in the area between curve A and B. In this area the efficiency of the engine, regarding fuel consumption and emissions, is measured in test cell. The engine is driven at constant speed and constant load (steady state) and measurements are done. Measurement points are marked with '*' in Figure 3.8. In the simulations, the combustion module senses actual engine speed, n, from the connected flywheel and reads information about fueling, δ, from the control unit. The output torque, T, can then be interpolated from the map

$$T = f(n, \delta)$$
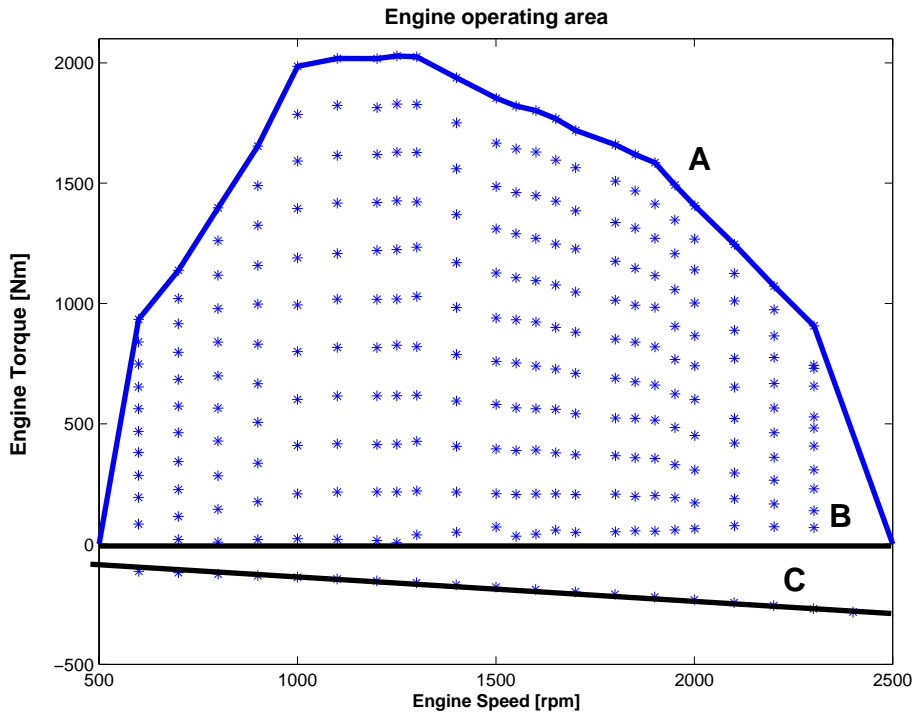
Figure 3.8: The engine produces power in the area between the maximum torque
curve A and the idle curve B. At curve C the engine is being dragged.

Fuel Consumption

The unit [g/kWh] is traditionally used by engine manufactures to describe spe-
cific fuel consumption since it is a convenient way to compare of the efficiency
of engines. This way of describing the engine performance works well when the
engine is producing power but not when the engine is dragging. This is the case
when the engine is at idle or when driving down a hill. When the power output
is zero the specific fuel consumption is infinity. This is illustrated in Figure 3.9.
It causes numerical problems in the simulation and would give very high fuel
consumption in terms of liter/100 km.

One way to solve this would be to change the fuel map so that the specific
fuel consumption is set to zero below a certain limit in load. The question
is where to set this load limit. Since the result of the total vehicle model
depends on where this limit is set this is not a good solution. For calculation of
fuel consumption another solution has been chosen. The control unit tells the
amount of fuel injected to the engine at every instance. Together with engine
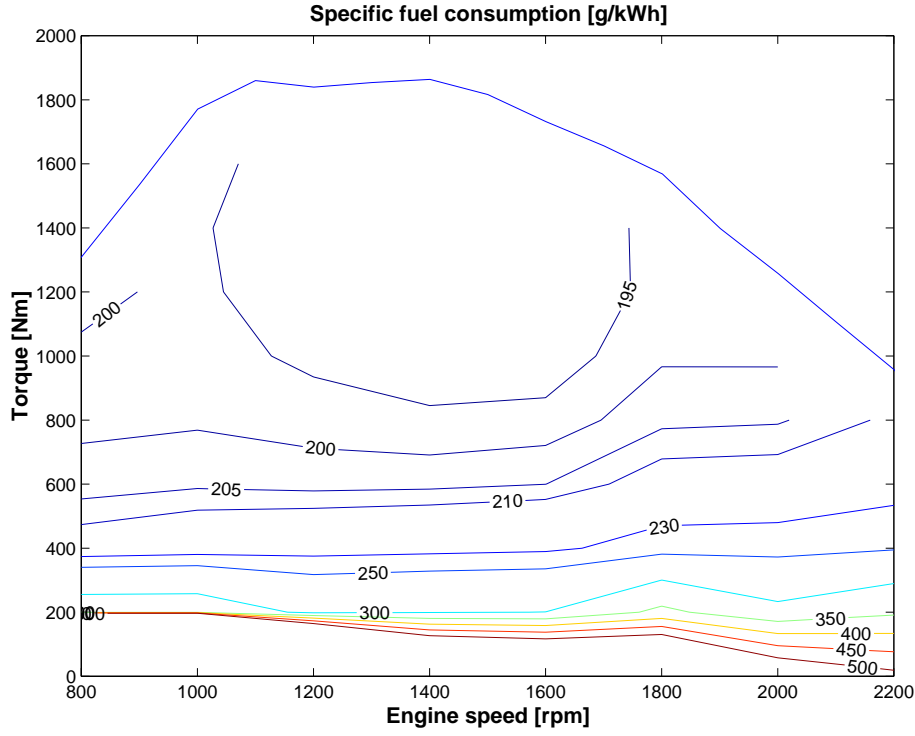
Figure 3.9: Fuel consumption described in g/kWh. It goes towards infinity at small loads and can cause numerical problems.

speed and number of cylinders the flow of fuel into the engine can be calculated

$$\dot{m}_{fuel} = n \cdot \delta \cdot \frac{z}{2} \cdot \frac{60}{1000} \qquad (3.6)$$

Here n is engine speed, δ is fueling and z is the number of cylinders of the engine. Integration of $\dot{m}_{fuel}$ over the simulation time gives the total amount of fuel used during the simulation

$$m_{fuel} = \int_{t_0}^{t_{end}} \frac{\dot{m}_{fuel}}{3600} \, dt \qquad (3.7)$$

The fuel amount, m_{fuel}, together with fuel density, ρ, and distance travelled, s, are then used to calculate fuel consumption in [liters/100 km]

$$\text{fuel consumption} = \frac{m_{fuel}}{\rho \cdot s} \qquad (3.8)$$

3.2.3 Exhaust Brake

Like all cars, trucks are equipped with service brakes (wheel brakes). In order to limit the wear of these, trucks are usually also equipped with an exhaust brake. The principle of the exhaust brake is to raise the pressure of the exhaust side of the engine. This can be realized in many ways but the most common way is to put a throttle in the exhaust system. By closing the throttle the exhaust pressure is raised and it gets harder for the engine to rotate and a braking torque is produced. The power of the exhaust brake, in absolute numbers, increases with higher speed of the engine, as can be seen in Figure 3.10.
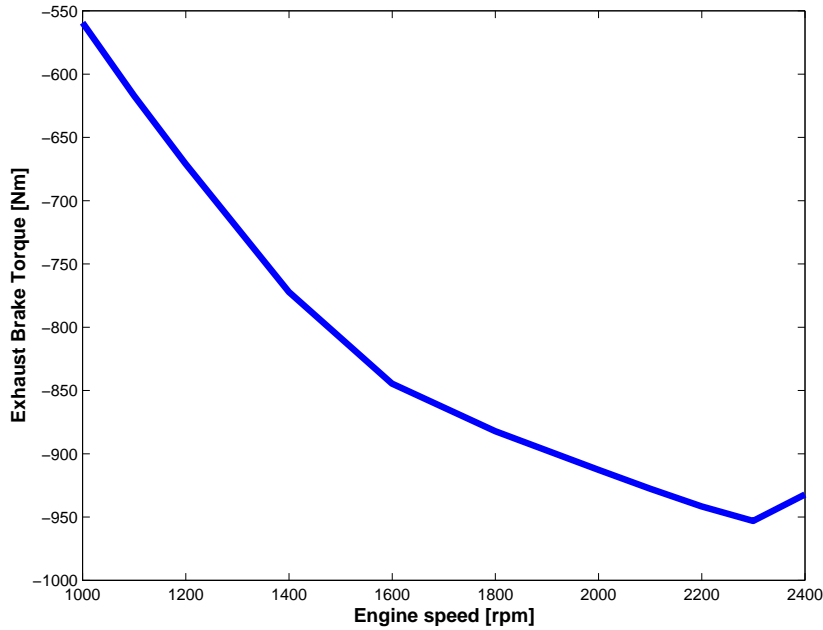
Figure 3.10: Exhaust brake torque, increasing absolute value with engine speed.

The exhaust brake module is implemented as a look-up table with exhaust brake torque as a function of engine speed. This negative torque is added to the torque from the combustion module to form the flywheel torque. The look-up table is based on measured values from test cell. A disadvantage with this approach is that engine friction is included twice. First in the engine module but it is also included in the measurement of the exhaust brake. Therefore when using the exhaust brake, the engine friction is also added. Engine friction is rather small compared with the exhaust brake torque and other external brake forces so this will not introduce any significant errors.

The exhaust brake can be on or off and is in this model controlled by the Retarder Control Unit (described in Section 3.3.3).

3.2.4   Auxiliary Units

Besides from propelling the vehicle, the engine also propel many auxiliary units. In a truck there are systems like air condition, servo steering, alternator, fan and air compressor for the pneumatic brake and suspension systems. All these systems require energy which is taken from the crankshaft of the engine. In reality, all of them are controlled mechanically and they are simply on or off. When they all are off, the load to the engine is constant at 24 Nm over the speed range. Activated, all except the fan and the alternator still show constant torque loads to the engine. For the alternator the load decreases slightly with increasing engine speed while for the fan the torque increases strongly with increasing engine speed. The maximum load from all the auxiliary units reach 270 Nm at 2000 rpm.

This means that the output torque from the engine to the wheels depend on which auxiliary units that are active. None of these systems gives any feedback to the control unit whether they are active or not. Due to this and the fact that no consumers are modeled the auxiliary units are simply modeled as one loss of torque, constant over the range of engine speed. This introduces an possible error to the model since load from the auxiliary units can be higher in reality.

3.3   Powertrain

Besides the engine, the powertrain consists of clutch, gearbox, retarder (optional), central gear, and shafts. This chapter describes these components, but to simplify the vehicle model the clutch and the shafts are not modeled. The gearbox is assumed to be of mechanical type.

3.3.1   Clutch

The function of a clutch is to synchronize engine speed and speed of the gearbox. This is used when the vehicle is started or when gear is changed. Events with slipping parts are very difficult to model properly and it requires a lot of numerical computation. These events only last a few seconds and therefore do not influence the overall fuel consumption when driving long distances. Due to these circumstances the clutch is not included in the vehicle model. Starts and stops are handled by introducing a minimum speed instead. For gear changes the ratio is changed instantly as described in the next section. This will decrease the computational time of the model, most likely without any influence in overall fuel consumption.

3.3.2   Gearbox with Opticruise

Mechanical gearboxes are dominating the market for heavy trucks, and therefore this type of gearbox is used in the modelling. The gear changing strategy is

important for fuel consumption. Vehicle simulation tools normally use a specified gear changing sequence, meaning that it always changes from 1st gear to 2nd and so on. The changes are then executed at predetermined engine speeds. This solution was not judged to be appropriate for models of heavy trucks since the weight can vary so much. A more flexible gear changing logic is necessary. Scania produces an automatic gear changing system, called Opticruise, that automatically selects and changes gear in a mechanical gearbox. The gear change is executed with engine control, so the clutch is only used for starts and stops.

For fuel consumption calculations, the short periods of time during gearshifts can be neglected compared to the long periods of driving. Therefore, a simple gear with constant ratio and efficiency is used to model the gearbox. Changing gear then means changing the value of ratio and efficiency. This is done instantly.
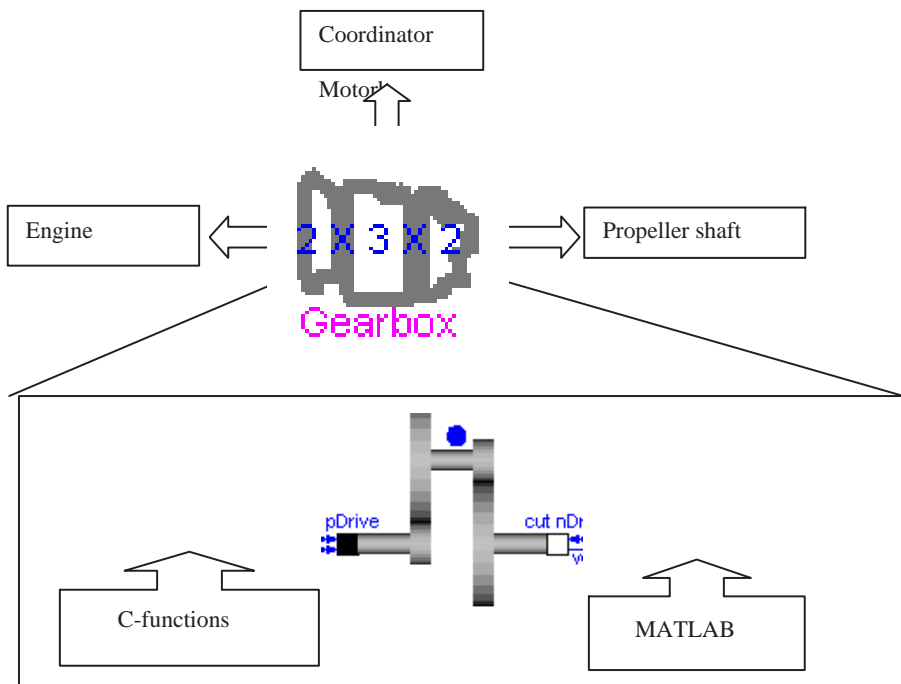
Figure 3.11: Gearbox module modeled by a simple gear in Dymola, a lookup table in Matlab and production C-code.

In the gearbox model, the next gear is calculated in an external C-file containing the gear selecting production code from the Opticruise system. This allows the gear to change 1, 2 or 3 steps up or down at every moment. The engine speed at a gearshift is not fixed; it varies with vehicle acceleration. A gear shifting sequence is shown in Figure 3.12. As can be seen, the gearbox in

this case first changes from 6th to 9th gear (3 steps up), a few seconds later from 9th to 11th gear (2 steps up) and then to the top 12th gear (1 step up). The lower part of the figure shows that no fix engine speed is used to execute gear change and the gear shift points are dependent on vehicle acceleration. For more information see (Tengroth, 1999).
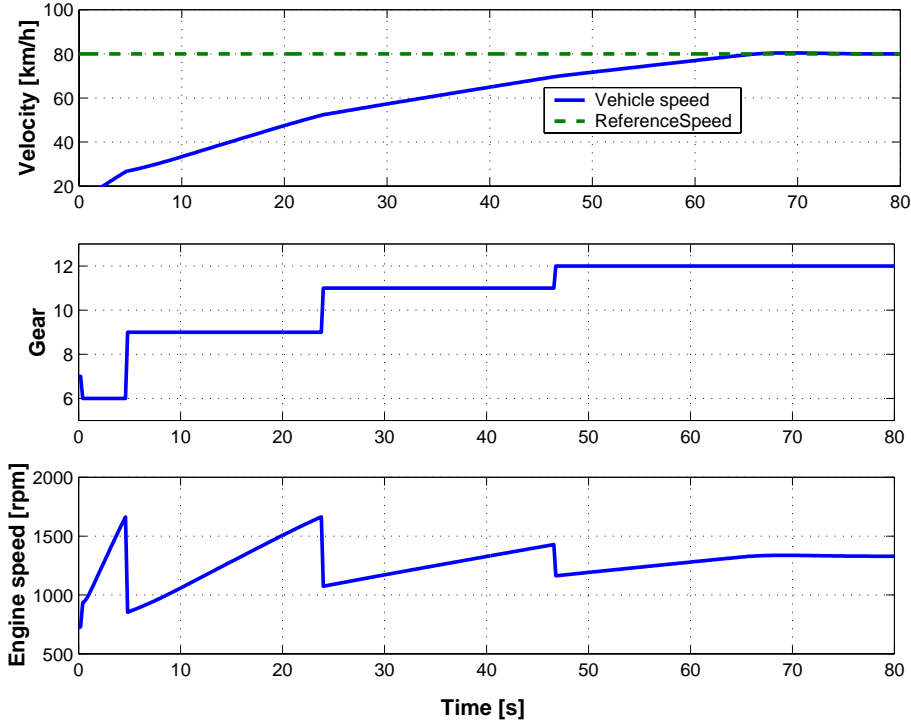
Figure 3.12: Gear shift sequence illustrating that the automated gearbox skips gears and execute gear changes at different engine speeds.

3.3.3 Retarder

Scania has a hydraulic brake system for longer continuous retardations like constant speed cruising down a slope. The system is called a retarder and it acts on the propeller shaft. The braking effort is achieved through forcing oil to rotate between two discs. The hot oil is cooled with water in a heat exchanger. This means that the ordinary cooling system of the engine is used to cool the brake energy away. The braking power of the retarder can be 300 kW continuously and up to 650 kW for short periods.

The retarder model is shown in Figure 3.13, consisting of a hydraulic part, control unit (RCU) and a cooling system for the engine. It is always used in
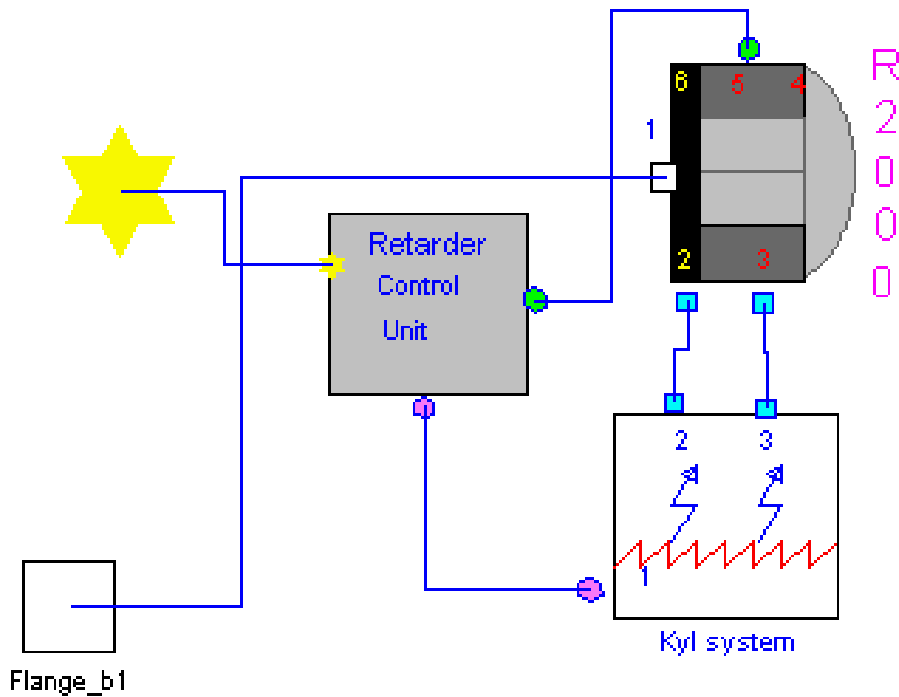
Figure 3.13: Retarder model with hydraulic brake, cooling system and control unit.

constant speed mode controlled by a PI-controller in an external C-file for an actual control system. The model also includes internal losses to form retarder drag. A known limitation is the fact that the engine model does not transfer heat to the cooling system. Instead the retarder model itself approximates this heat transfer with a constant value. This means that the thermal limit of the retarder model is not modelled. The retarder model is described in detail in (Kjell and Asplund, 1999).

3.3.4   Central Gear

The central gear, also called final gear, is a hypoid gear used to divert torque to the two driving wheels. It also has a differential allowing the two wheels to rotate with different speeds in cornering. Since the vehicle model is restricted to longitudinal motion (no corners) the differential is not necessary. This also allows the whole axle to be symbolized with one wheel only. A single gear, illustrated in Figure 3.14, with the two parameters ratio and efficiency therefore models the central gear.
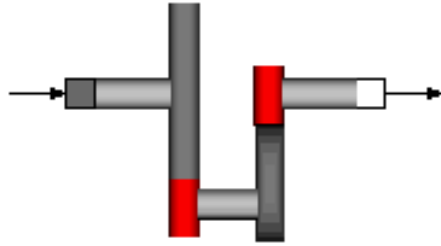
Figure 3.14: Final gear in powertrain library modeled by a gear without differential.

3.3.5 Shafts

To transfer power between the gearbox and the central gear and further to the wheels a propeller shaft and a drive shaft are needed. The propeller shaft is designed with the lowest break stress since it is easiest to change. The drive shaft is the least stiff part of the powertrain, and it may introduce oscillations of the first order (Pettersson and Nielsen, 1997). These oscillations do not affect fuel consumption and non-of these components are therefore included in the model. The whole powertrain is thus modeled rigid.

3.4 Wheel

The wheel is the contact between the chassis, the ground and the powertrain. It transfers the torque from the powertrain to the ground and the resulting tractive force pushes the chassis forward. In longitudinal motion, wheels are affected by two main phenomena of tires: rolling resistance and slip. Due to the large weight of trucks, the largest resistance force on the truck on flat road is the rolling resistance as seen in Figure 2.2. Therefore, wheel models with good expressions for rolling resistance is important in fuel consumption calculations. This section describes the effective rolling radius of a tire, its rolling resistance and slip.

3.4.1 Effective Rolling Radius

When a vertical load is applied to a wheel the tire is compressed in the area of ground contact. This means that the tire is no longer a perfect circle since a part of it is flattened by the ground. The vertical load also causes the distance between wheel center and ground (loaded radius) to become smaller than the free radius of the wheel.

In (van Eldik Thieme, 1971) the effective rolling radius, R_e, is defined as the ratio of the linear velocity V of the wheel center in the longitudinal direction

to the angular velocity ω of the wheel

$$R_e = \frac{V}{\omega} \tag{3.9}$$

The effective rolling radius is often erroneously assumed to be equal to the center height or so called loaded radius R_l, being the distance from the center of tire contact to the wheel center. When R is the undeflected free tire radius, it can be shown that:

$$R_l < R_e < R \tag{3.10}$$

that is, the rolling tire travels farther per revolution than determined by using its center height as rolling radius, but less than described by the free tire radius. This is illustrated in Figure 3.15.
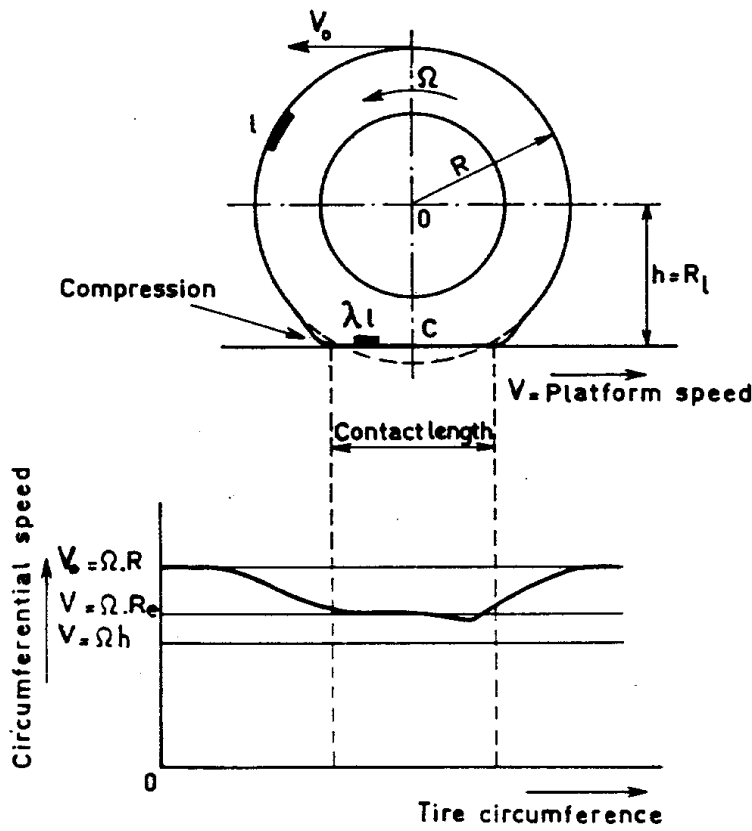
Figure 3.15: Circumferential speed of a tread element when passing through the contact zone. The figure is obtained from (van Eldik Thieme, 1971).

An increase in load at constant pressure results in a larger deflection of the tire. Due to an increase of the compression of the tread, the effective radius is decreased. At higher speeds the tire will grow, due to larger centrifugal forces, resulting in an increase of effective radius R_e, increase of loaded radius R_l and an increase of free radius R. This effect mainly occurs on bias ply tires and is almost negligible for the radial belted tire. Today, mainly radial belted tires are used on passenger cars and trucks.

In this work, data from the tire manufacturer Michelin is used. They claim that for heavy truck tires the effective wheel radius increases by 2% with speed up to 30 km/h and thereafter remains constant over the rest of the speed range.

3.4.2   Rolling Resistance

The rolling resistance of a free rolling tire is mainly caused by hysteresis in the tire materials which occurs during the cyclical deformations when the wheel is rolling. Friction between the tire and the road caused by sliding, the resistance due to air circulating within the tire and the fan effect of the rotating tire on the surrounding air also contribute to the rolling resistance of the tire but they are of secondary importance. According to (Wong, 1993) 90-95% of the rolling resistance is caused by internal hysteresis, 2-10% by friction between the tire and the ground and 1-3% is caused by air resistance.

Methods of Measuring Rolling Resistance

(van Eldik Thieme, 1971) presents three ways to measure the rolling resistance on the road.

- Towing a vehicle at constant speed.

- Allowing a vehicle to coast and measure the rate of deceleration.

- Measurement of the torque in the drive shaft of the vehicle required to maintain its speed.

It is stated to be difficult to find the rolling resistance accurately from these test, because it is not easy to separate other friction from measured results. The later approach is though used and presented Chapter 5 in this work.

Practically all measurements of rolling resistance are done by loading the tire against a smooth steel drum. For truck and bus tires, measurement procedures are described in ISO standard 9948. A typical view of the arrangement is shown in Figure 3.16. The speed of the drum keeps the tire at a speed equivalent to 80 km/h. The tire is loaded to 85% of maximum load and has the correct air pressure. After 5 hours of rotation indoors at 25 °C the rolling resistance is measured. The wheel is mounted with special bearings so that no losses in the bearings affect the measurement.
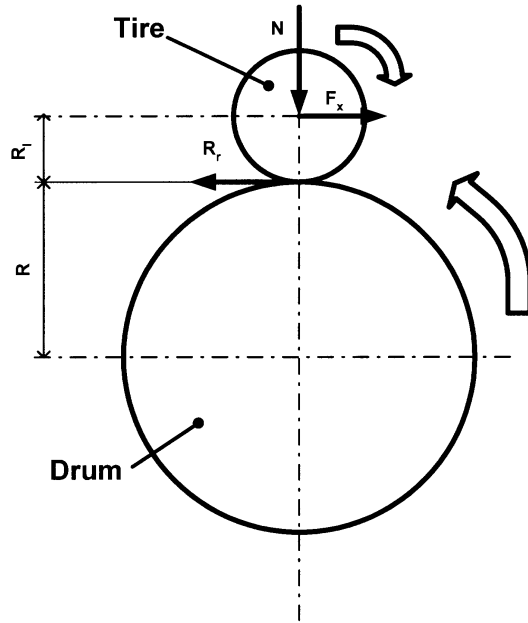
Figure 3.16: Measurment of rolling resistance on a drum.

The rolling resistance is proportional to the normal force acting on the wheel.

$$R_r = C_r \cdot N \qquad\qquad (3.11)$$

A typical value of the coefficient of rolling resistance, C_r, for trucks is 0.07 kg/ton. Passenger cars usually have values twice that big. The difference depends on other tread rubber compounds, higher inflation pressure and radial stiffness for truck tires.

Due to the curvature the value of C_r from the test drum must be corrected to fit applications on flat road. This is also described in ISO9948. For a typical truck tire the value of C_r decreases about 9% when moving the tire from the drum to a flat road.

Factors Influencing Rolling Resistance

Since the rolling resistance of a tire primarily is caused by hysteresis in the tire material it is strongly dependent on the deflection of the tire and the rotational speed. As mentioned above, the deflection depends on the vertical load and the inflation pressure. It decreases with increasing air pressure in the tire and increases with increasing load. The hysteresis and rolling resistance are also affected by the tire temperature since a warm tire knead more easily. Of course, also the road conditions influence.

Incorrect wheel adjustment can give higher rolling resistance. In the model, tire air pressure and wheel adjustments are said to be at rated values. The rolling resistance is also dependent of the ambient temperature, but ISO 9948 only support temperatures between 20°C and 30°C. Corrections for ambient temperature is therefore not implemented in the model.

Speed Dependence

The coefficient of rolling resistance also depends on the speed of the vehicle. Based on experiments with radial-ply truck tires (Wong, 1993) claims the coefficient of rolling resistance to increase with the square of the speed

$$C_r = 0.006 + 0.23 \cdot 10^{-6} \cdot v^2 \tag{3.12}$$

Here v is the speed in km/h. The expression is said to be valid up to 100 km/h.

The tire manufacturer Michelin, has proposed the following formula

$$C_r = C_{riso} + a \cdot (v^2 - v_{iso}^2) + b \cdot (v - v_{iso}) \tag{3.13}$$

which is used to account for the effect of speed on the coefficient of rolling resistance in order to estimate C_r at other speeds following initial measurements at ISO9948 conditions. C_{riso} = value from measurement according to ISO9948 [kg/ton]. v_{iso} = 80 km/h, speed during measurement according to ISO9948, a and b are constants. This expression is valid between 0-90 km/h and is together with Equation (3.12) shown in Figure 3.17. These expressions show very different qualitative properties at lower speeds. From Michelin values of C_{riso} can be delivered for different types of tires and treads. Since these values are in accordance with the ISO standard Equation (3.13) is used in the wheel model. Both these expressions are based on stationary conditions of the tire. The difficulties with this type of model will be discussed in Chapter 5 followed by a new dynamic model for rolling resistance in Chapter 6.

3.4.3   Traction and Slip

The previous discussions about wheel and tire are all valid for free rolling tires. This part describes what happens when a tractive torque is applied to the wheel, a phenomenon of tires called slip. It is described even though it is not used in the vehicle model for the fuel consumption calculations. The main reason is that slip is considered to be low when driving at cruising speed and that it does not influence fuel consumption much. For a typical truck on a flat road at 80 km/h slip is about 0.8%. An introduction of slip in the wheel model would also require knowledge of the coefficient of road adhesion for the different roads used. This knowledge is not always available and does also vary with weather conditions. Adding slip also means adding one more degree of freedom to the model, and this could be a possible drawback since it would require one more state variable of the powertrain and could increase the computational time for the model.
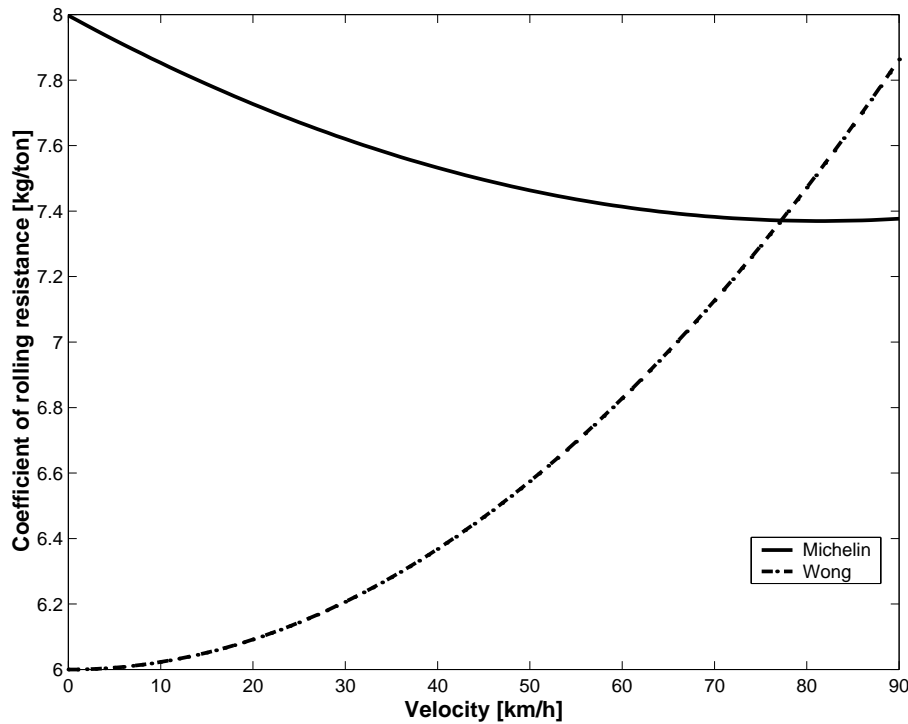
Figure 3.17: Coefficient of rolling resistance as function of speed. Two different approaches.

When a driving torque is applied to a pneumatic tire, a tractive force is developed at the tire-ground contact patch as shown in Figure 3.18. At the same time, the tire tread in front of and within the contact patch is subjected to compression. A corresponding shear deformation of the sidewall of the tire is also developed. A compressed tread element adheres to the ground when first entering the contact zone. As it moves further the increasing deflection of the tread element produces a linearly increasing longitudinal force. Beginning in the rear part of the contact zone, forward sliding of the tread element will be observed. The resulting longitudinal sliding distance and sliding velocity are also shown in Figure 3.18.

This compression due to tractive torque decrease the effective radius. (A braking torque increase the effective radius.) The effective radius is defined such that the slip velocity is zero for free rolling.
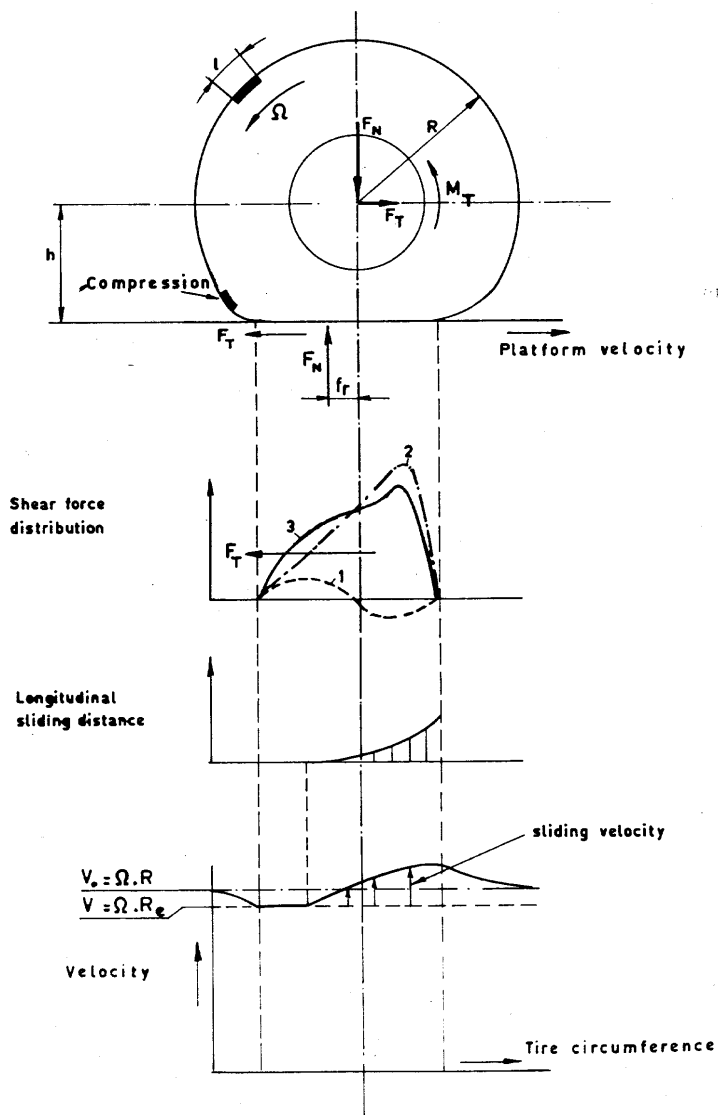
Figure 3.18: Behaviour of a tire under the action of a driving torque. The figure is obtained from (van Eldik Thieme, 1971).

Definition 1. *The slip ratio is defined to be:*

$$slip = \frac{\omega_T - \omega_0}{\omega_T} = \frac{R_{e0} - R_{eT}}{R_{e0}}$$

where ω_0 = angular velocity at free rolling and ω_T = angular velocity with traction.

Another definition of slip can be found in the *SAE Handbook Supplement, Vehicle Dynamics Terminolgy J670e*: $slip = (R_{e0} - R_{eT})/R_{eT}$. Both definitions give a positive value of slip from tractive torque. The SAE definition is formulated with ABS braking systems in mind, avoiding division by zero for locked wheel ($\omega_T = 0$). Definition 1 is favorable when starting from standstill. The decrease in effective radius R_{eT} compared with the free rolling case may be obtained by measuring ω_T and ω_0 at constant drum speed.

As the tractive force developed by a tire is proportional to the applied wheel torque under steady-state conditions, slip is a function of tractive effort. At first the wheel torque and tractive effort increase linearly with slip because, initially, slip is mainly due to elastic deformations of the tire tread. A further increase of wheel torque and tractive force results in a part of the tire tread sliding on the ground. Under these circumstances, the relationship between the tractive force and the slip is nonlinear. Based on experimental data, (Wong, 1993) states that the maximum tractive force of a pneumatic tire on a hard surface is usually reached somewhere between 15 and 20 % slip. This maximum is reached at the peak (static) value of the coefficient of road adhesion. For larger values of slip the tractive effort levels out at the sliding (dynamic) value of the coefficient of road adhesion. This relation is shown in Figure 3.19.
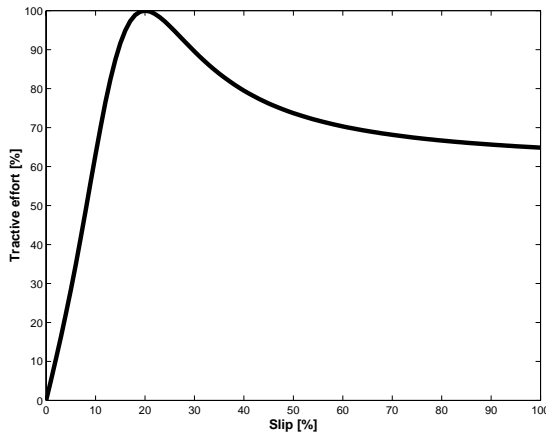
Figure 3.19: Relation between relative traction force percent and traction percent slip.

A well known analytic expression regarding slip is the "Magic formula" presented by (Pacejka and Bakker, 1993). This is an empiric formula based on measurements, where there are also versions for calculating longitudinal or lateral force due to longitudinal or side slip. A modified version also exists that can be used for combined longitudinal and side slip (Bayle et al., 1993).

3.4.4 Bearing Losses

All wheels are mounted on bearings. Due to internal friction energy is lost in the bearings. According to the *SKF handbook* the losses mainly depend on the load of the axle

$$T_{bearing} = N \cdot \mu \cdot \frac{d}{2} \qquad (3.14)$$

where N is the load on the bearing, μ is the internal friction of the bearing, d is the inner diameter of the bearing and $T_{bearing}$ is the torque of resistance. The losses are proportional to the load on the axle.

3.4.5 Number of Axles

As stated above, both rolling resistances of tires and wheel bearing losses are proportional to the axle load. This means that the number of axles does not influence the total resistance force, only the total weight. In practice, a common opinion is that energy losses increase with the number of axles. This is not the case in this model but in practice the risk of wrong air pressure in some tires or wrong wheel alignment do increase with the number of axles. In the model, these things are always at rated values.

3.4.6 Wheel Model

In Figure 3.20 the used wheel model is shown. Rolling resistance and losses to the wheel bearings are included but not slip as explained above. The point of action for rolling resistance, R_r, is set to the center of the wheel which is equivalent to treating the rolling resistance as a pure braking torque. In the equations below the equilibrium for the wheel is shown.

$$
\begin{aligned}
F_x - R_r + F_{tractive} &= 0 & (3.15) \\
F_y + N &= 0 & (3.16) \\
T - F_{tractive} \cdot r - T_{bearing} &= 0 & (3.17)
\end{aligned}
$$
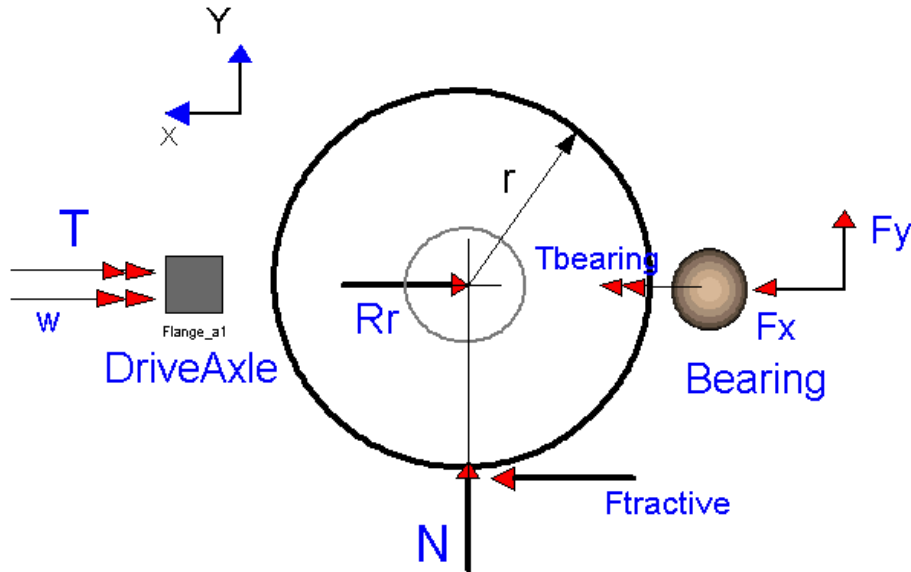
Figure 3.20: Forces on used wheel module.

3.5   Driver and Brake Control

A model of the driver is difficult since no standard equations exists to describe the drivers behavior at all times. As mentioned earlier, the driver model has partly been replaced by automatic systems like cruise control for speed control and Opticruise for gear shifting. Here the driver model has a monitoring function. The driver model looks ahead on the road to see changes in slope and reference speed. It looks a few seconds in front of the vehicle, meaning that the distance that it looks forward increase with increasing vehicle speed. This look ahead means that the reference speed ahead of the vehicle is used. In Figure 3.21 this is illustrated, the cruise control sets the fuelling to zero approximately 160 m before the reference speed drops from 70 km/h to 50 km/h. When travelling in 70 km/h, an advance of 8 seconds is approximately 160 m. After a while the speed has dropped to 50 km/h and the fueling is raised again.

Brake Systems

When driving a heavy vehicle down a hill the weight tends to push the vehicle speed up. To be comfortable, the driver would like a constant speed down a hill. Trucks today normally have 2 or 3 different brake systems to realize this; service brakes acting on the wheels, exhaust brake acting on the engine and, optionally, a retarder acting on the propeller shaft. Exhaust brake and retarder

Figure 3.21: The driver looks ahead on the road. The fueling to the engine is dropped before the vehicle reaches the position with lower reference speed. When the speed has dropped to the new reference the fueling is raised again.

does not wear like service brakes and does not require maintenance. Another problem with service brakes is that they can lose their effect (fade) if they get to hot. This problem is most severe if the brakes are of the drum type. Disc brakes are not that sensitive due to better cooling. Due to these facts truck drivers use the exhaust brake or the retarder first, and only when that is not sufficient the service brakes are activated.

Since a retarder is an option, the model must be able to function both with and without it. The problem is solved by always including the retarder and introducing a logic variable "Retarder" in the driver module. If the retarder shall be used in the simulation the logic variable is set to 1 else to 0. The output torque from the retarder model is then multiplied with the logic variable (1 or 0 depending on the choice). This also includes the retarder drag.

Schwung

Schwung is a value of the velocity that the driver allows when driving down
hill. It is a form of energy saving since the driver allows the vehicle to reach
a higher speed when going down hill and the engine has stopped to produce
energy. This kinematic energy stored in the vehicle can be used to travel some
distance after the hill without giving fuel to the engine. Usually schwung is
rather small, 5-10 km/h above the cruising speed on flat road. In the model the
exhaust brake and/or Retarder are activated if the velocity increases above this
limit. If the hill is steep or if the exhaust brake alone not is powerful enough
and the velocity continues to increase the service brakes are activated. This is
shown in Figure 3.22 illustrating a truck (total weight 40 ton) going down a 3%
slope. The engine produces energy up to the level of the reference speed, if the
velocity increases above the level of schwung the exhaust brake is activated as
seen in the 2nd part of the figure. If the velocity still increases and passes the
speed limit, the service brakes are activated as illustrated in the third part of
the figure. The service brakes are powerful (in this work modeled as a braking
force equivalent to a retardation of $0.1g$) and reduces the speed down to the
schwung limit again.
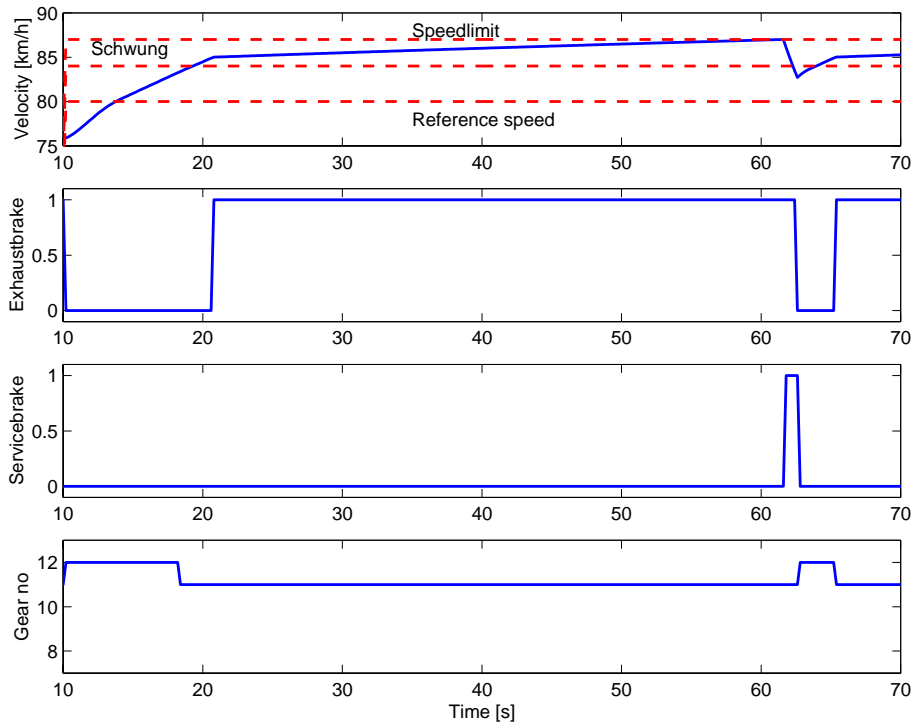
Figure 3.22: Activation of different brake systems at different levels of speed.

3.6 Ambient

The ambient conditions to the vehicle model has two parts; the road and the weather. The model of the road describes the longitudinal road in terms altitude and slope. It also contains a reference speed that the vehicle model should follow. The weather model simply describes the state of the air pressure and air temperature around the vehicle.

3.6.1 Road

To be able to simulate vehicles in different environments Scania has a database of recorded road profiles. It contains roads from all over the world. Using the road profiles in the simulation program allows various kinds of vehicles to be simulated on a road profile from their respective country. This is useful and makes the simulations of different transports more realistic. Roads can be recorded by driving the actual road with special equipment in a vehicle. The equipment records distance, speed and altitude and is described further in Chapter 7. A typical road profile is shown in Figure 3.23.
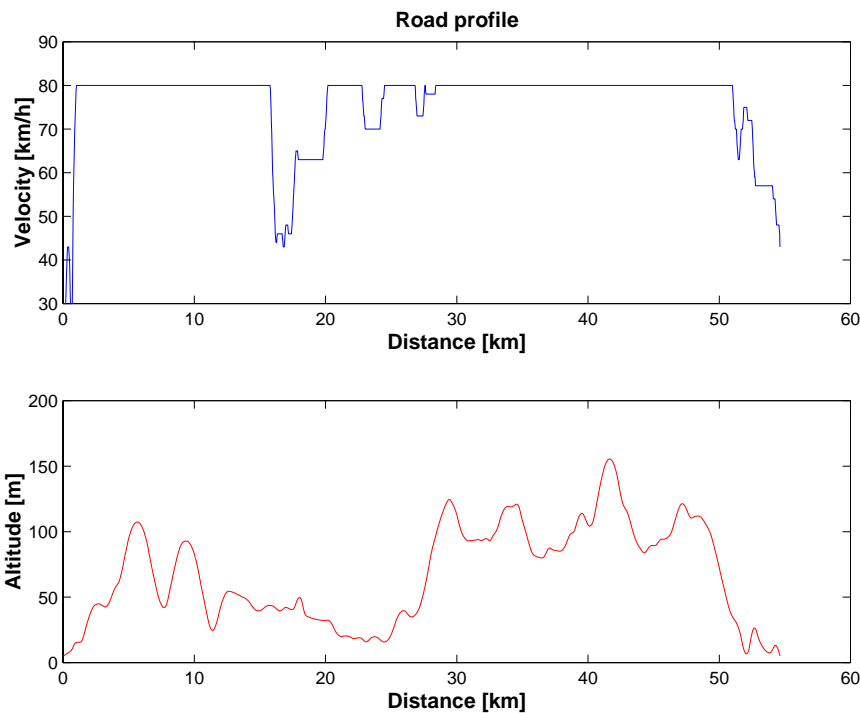
Figure 3.23: Road profile. The recorded velocity is used as reference in the simulations. The altitude is recorded to calculate the slope.

Data about the recorded road are stored in tables for altitude and reference speed dependent on the distance. They are complemented by a table for the slope of the road calculated as the derivative of the altitude, this will be described in Chapter 7. The reference speed is used as reference value in the speed control systems, cruise control and retarder. The slope is used to calculate the resistance force in all masses due to the inclination of the road.

3.6.2   Weather

The model weather is used to set conditions like air temperature and air pressure, that are used to calculate air density. The parameters are held constant during the simulation. (They are now used only for air resistance only but could also be used by e.g. the engine.)

4

Simulation

The model from Chapter 3 is in this chapter implemented in an object-oriented language. It uses production code together with exchangeable data sets to perform fast simulations of any truck from the production range. This is combined with a graphical user interface to form STARS (Scania Truck And Road Simulation), a simulation program used to calculate fuel consumption for a truck on a road recorded somewhere in the world. The chapter starts by stating the user requirements in Section 4.1. In Section 4.2 the design requirements on, and selection of, a simulation tool are stressed. This is followed by a presentation of the implemented vehicle model in Section 4.3. Finally, the main result, STARS is presented with its graphical user interface.

4.1 User Requirements

As stated in Chapter 2 there are several users of a simulation program for fuel consumption. Some users want to predict fuel consumption for trucks operating on the highway. This information can be used to study their environmental performance, cost calculations etc. Others want to use the program to develop production code for the control of the engine and the gearbox used in the model. The main planed application for the program is to compare the impact of different powertrain configurations on fuel consumption. This requires the simulation program to have an easy to use graphical user interface and possibilities to specify the production range of powertrain components.

4.2   Design Requirements

This section describes all the requirements on the simulation tool. They are
modular design, exchangeable data sets and the use of production code within
the model. To be able to compare different powertrain configurations within a
few hours the simulations need to have short execution times on a standard PC.

4.2.1   Modular Design

Creating models of the kind used in this work is time consuming, and the val-
idation of them even more. Therefore it would be advantageous if the models
could be reused for other simulations in the future. One way to achieve this is
through modular design meaning that every component is modeled and stored
in a component library. To be modular it should also be independent of the
computational causality and use a standardized interface towards other compo-
nents.

   One advantage with a model component library is that it promotes reuse
of models, another is that it can be built with modules of varying complexity.
This is useful when developing a model since one can start with a simple model
and when it is functioning add more complexity. Different modules can also
be used for different purposes, for instance, when calculating fuel consumption
over long time of highway driving, a simple model of the engine is needed. If
studying engine warm up, a more detailed engine model with heat transfer and
cooling system is required. The modularity also makes it possible for experts
in different areas to work with modules in their specialized field independently
of others. This contributes to a better and possibly a more detailed model.

   These things are illustrated in the wheel library in Figure 4.1 which contains
three different wheel models of different complexity. Wheelsimple does not
include slip or rolling resistance, Wheel1 include functions for rolling resistance
and Wheel2 also includes expressions for wheel slip. They are all based on the
common base class Wheelbase that defines the standardized interfaces towards
the chassis and to the rest of the powertrain. This means that any of these
three can be used for simulations and that they are exchangeable by just "drag
and drop".

Figure 4.1: Wheel library, several exchangeable modules of different complexity.

4.2.2 The Need for Exchangeable Data

Modular design gives a flexibility to build several models by combining components in different ways. This is very useful but sometimes it is also necessary to use the same model and study variations of different settings of variables. As stated in Chapter 2 one main purpose with the simulation program is to study the influence on fuel consumption of different powertrain configurations. To change the value of a single constant or parameter is normally easy to do. But to change type of engine it is necessary to change several maps describing torque production and emissions. The same situation goes for the road profile and the gearbox, which also needs large data sets. In order to allow simulation of different engines, road profiles and gearboxes it is necessary to have an easy way of exchanging modules of data in the simulation tool.

4.2.3 Use of Production Code

Creating a computer model of the mechanics in a vehicle is fairly simple because the equations describing the physics are known well enough. A much harder problem is to make a correct model of the control systems in the vehicle and of the driver. Very little theory exist on how to describe the behavior of drivers in different situations. One solution is to use the many support systems that exist to assist the driver in real vehicles. As described in Chapter 3 the function of the cruise control and the Opticruise system are desired in the model. This can be done by including the source code originally written for these systems in the computer model.

The advantages of using production code are more accurate results, shorter modeling time, and the possibility to develop these systems further. This requires the model to use the same signals and variables as in reality. It also requires the simulation tool to have the possibility to read external source code files.

4.2.4 Selection of Simulation Tool

The requirements on the simulation tool can be summarized as:

- Fast simulations of long driving distances.

- Allow a modular design.

- An easy way of exchanging modules of data.

- Manage external source code.

The software tool selected for the vehicle model is Dymola (Elmqvist et al., 1996). It uses the object-oriented language Modelica (Elmqvist and Mattson, 1997) and has an equation-oriented concept (i.e. non-causal modeling). Modelica is a standardized modeling language and it supports different formalisms

like ODE (Ordinary Differential Equations) , DAE (Differential Algebraic Equations), bond graphs, finite state automata and Petri nets.

With Dymola it is easy to build modular component libraries and it is possible to include external C or Fortran files. Dymola is a 3rd part supplier to Matlab and uses its format for data files in both the generated result file and for the input file with data tables (maps). The exchange of large data sets can therefore be managed from Matlab.

Upon entering the model, Dymola instantiates all submodels (objects) from the model types (classes). It extracts the formulated equations from these objects. The whole system of equations is then sorted into computational order and unknowns are solved algebraically from the equations. The equations of the model are as far as possible solved algebraically and only when the system contains simultaneous equations (i.e. algebraic loops) they are solved numerically. The solved equations are then translated to C code and compiled. This allows both easy programming and fast simulation times.

It can be concluded that the simulation tool Dymola fulfills the requirements set up for this work.

4.3   Longitudinal Vehicle Model

All the models described in Chapter 3 are implemented in Dymola, organized in a component library structured in accordance with Figure 3.1. All the components can be combined to form a complete vehicle model as shown in Figure 4.2. This model has two masses, one in the chassis and one in the cargo. They are rigidly connected to each other through the trailer module. In this model the same wheel model is used in all three positions independent of the wheel should be driven or not. A driven wheel has torque as input while a free rolling wheel has speed as input. This is possible since the modules are non-causal.

In the real vehicle there are many complex signals going from one control unit to another. The same situation appeared when creating this vehicle model. To avoid to many lines and connections the model Coordinator was created. The Coordinator collects signals from most of the modules and makes the signals available for other modules. The only calculation done in the Coordinator is conversion of speed [m/s] to velocity [km/h].

To achieve the correct speed of the vehicle model it is controlled by two control systems. For positive acceleration the cruise control in the engine is used. For negative acceleration the speed control of the retarder brake is used. This function also controls the exhaust brake of the engine. If this brake effort not is enough, the driver model can activate the service brakes. A constant brake force is then applied to the vehicle.

This model has two state variables, the position and the speed of the vehicle. It consists of 564 equations with 79 parameters. The model is simulated with a 0.2 second fix step Runge-Kutta algorithm. To simulate a truck driving a road distance of 100 km takes 100 seconds on a standard PC (300 MHz). Different
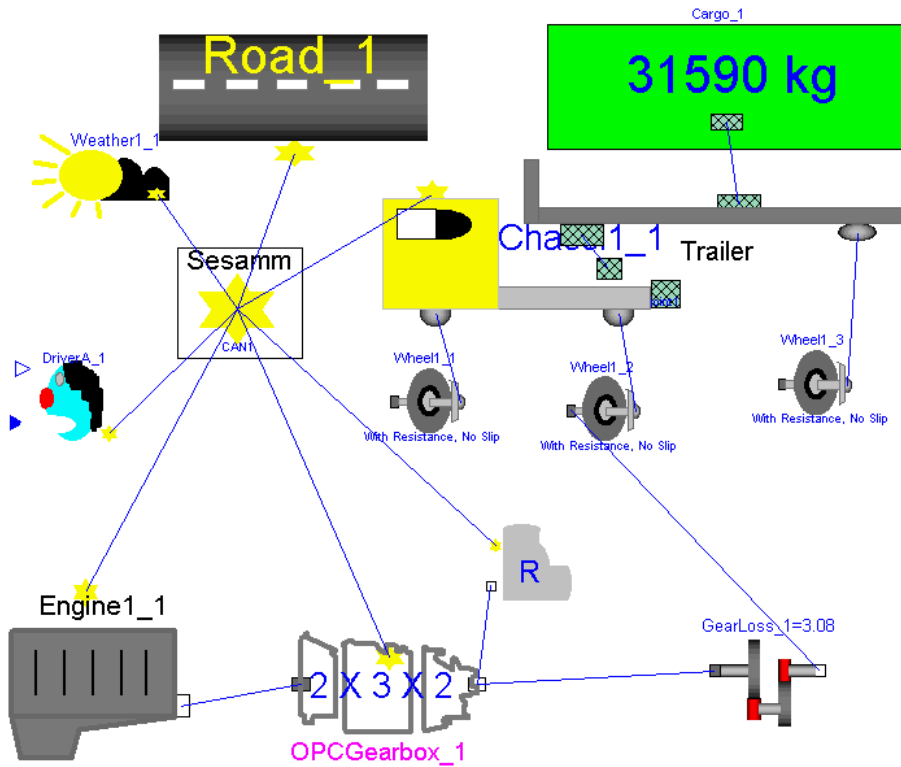
Figure 4.2: Complete vehicle model used for fuel consumption simulations of a heavy truck in highway driving.

numerical solvers are tried also. With a multi-step solver called DASSL the simulation takes 22 times longer CPU-time. Any difference in the results (fuel consumption, average speed etc) are hardly noticeable. The big difference in CPU-time depends on how Dymola handles included production code. The production code is written for a specific constant sampling rate of 20 Hz. In the model it is scaled to 5 Hz and to ensure a constant sampling rate its evaluation is wrapped with a when-sample routine. This makes it possible to use other simulation rates and still ensure that the production code is evaluated at the right occasions. The problem with the multi-step solver is that it sees the evaluation of the when-sample routine as an event. At events this kind of solver stops, goes back in time and continues with smaller steps towards the event. These small steps is the reason for the long CPU-time required. These problems could be avoided if Dymola did not treat the evaluation of the when-sample routine as an event.

4.4   STARS

With Dymola it was possible to create a suitable vehicle model but in order to make it easy to use a graphical user interface (GUI) is needed.

Since Matlab is required to manage the exchangeable data sets it has also been used to build the GUI. From the GUI it is possible to change all parameters, initial values and data sets used in the model. This means that after compilation of the model in Figure 4.2 in Dymola it is possible to create a stand alone application in Matlab controlling all inputs to the simulation. This application is called STARS (Scania Truck And Road Simulation). It is also used to start the simulation and view the results from it.

Selection of Road

The data selection part of STARS is shown in Figure 4.3, here one of the 300 different road profiles from all over the world can be selected. It is also possible to view this road graphically, to change the maximum speed and to zoom in and just choose a small part of the road for simulation. In the simulation program it is desired to simulate a certain distance of a road but the simulation tool is time based. This has been solved by introducing the parameter "maxdistance" in the road model. In the GUI the length of the road is read from the road file and assigned to the parameter. When the simulation reaches the maxdistance a model error is executed and simulation is stopped. The ordinary simulation stop time must be set to a high value otherwise the simulation will stop before reaching the end of the road.
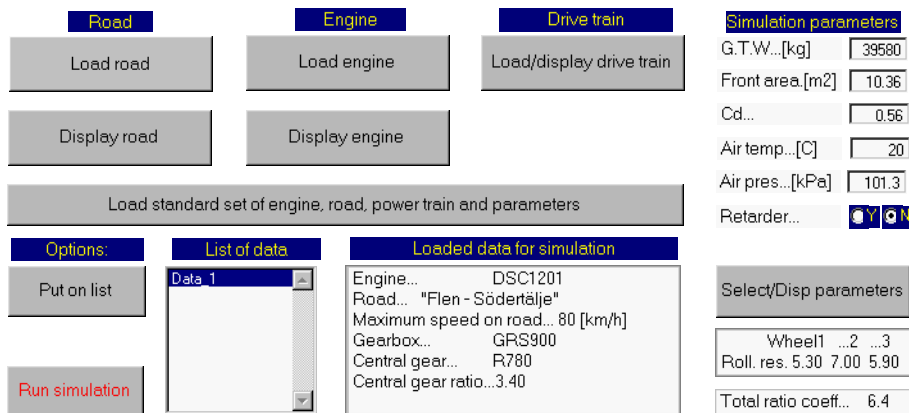
Figure 4.3: Graphical user interface in STARS for specifying input data.

Powertrain Selection

In STARS is also possible to choose from around 30 types of engines. Their fuel and emissions map can be studied together with maximum power and torque curves. For the rest of the powertrain it is possible to choose between a 12 speed or a 8 speed gearbox and combine it with one of the numerous final gear ratios. It is also possible to choose if the Retarder should be used in the simulation or not. Many different tire dimensions with different treads can be chosen from. Other parameters that are possible to change are the weight, the frontal area, the coefficient of air resistance, air temperature and air pressure.

Data for the road and the engine are described in several maps and are good examples of exchangeable data sets as discussed in Section 4.2.2. All the maps used have names predefined in the model. To change for instance engine, data is loaded into Matlab's workspace and saved to the file "dsdata". This is the file that Dymola interpolates in during simulation.

The GUI is also used to start the simulation of the model and to evaluate results.

Presentation of Results

The result file from the simulation is loaded in to Matlab, processed and presented. The GUI is used to make calculations, after a simulation, which are not based on time. These are calculations like fuel consumption in liters/100km or statistical calculations of operational points. In Figure 4.4 values of fuel consumption, distance, average speed etc are shown in the upper left corner. Below, the used input values like engine type, road and weight are displayed. To the right the simulated speed is compared with the reference speed and below the altitude of the road is shown.
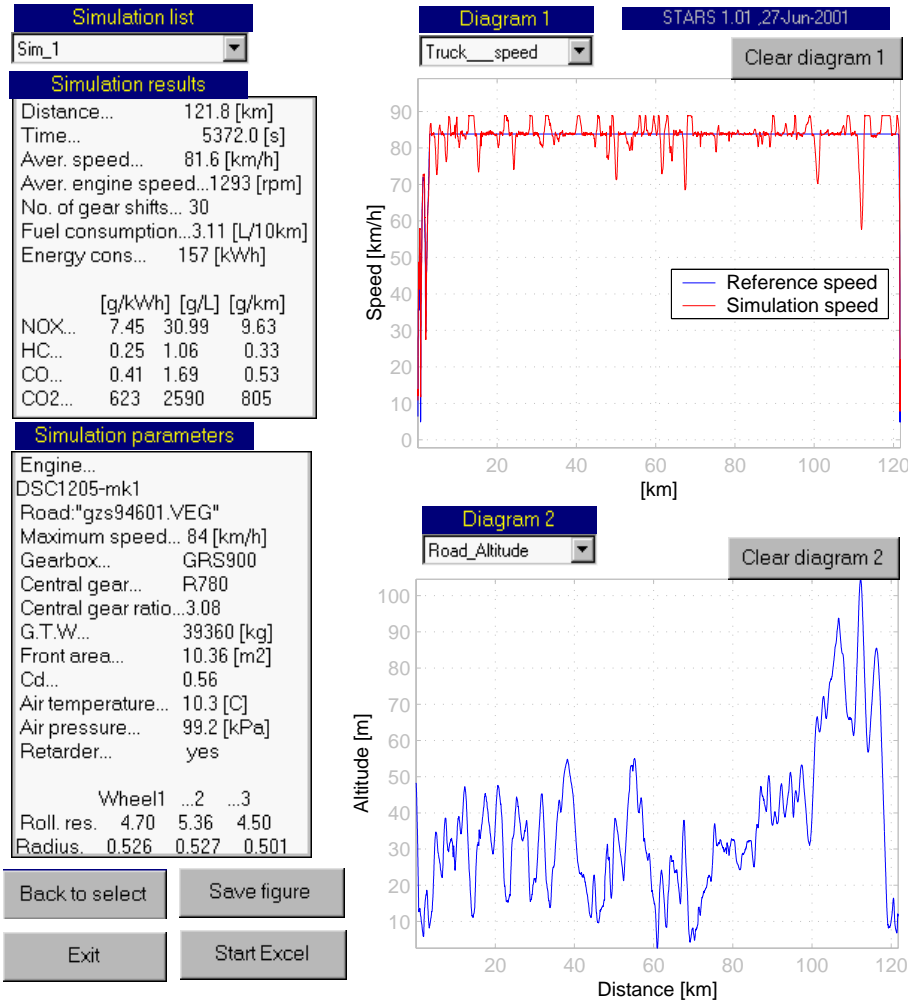
Figure 4.4: Result window in the simulation program STARS.

Validation of Energy Losses

To validate the model presented in Chapter 3 and illustrated in Figure 4.2 several experiments are necessary. This chapter presents experiments to validate energy losses like rolling resistance and air resistance. The validated parts of the vehicle model are encircled in Figure 5.1. The validation is done by driving a known vehicle at constant speed on a road with constant slope while measuring torque on propeller shaft, fueling to engine, engine revolutions and vehicle speed. Tests at different speeds are used to identify forces of rolling resistance and air resistance. (Blumberg, 1976) has earlier presented similar work for passenger cars. Blumberg measured torque on the drive shafts when driving a vehicle in steady-state speeds. The purpose was to create a powertrain model, with a correct load on the engine, to be used for development of engine control strategies in engine test-cell.

The measured propeller shaft is used to adjust a traditional model for rolling resistance. The match is reasonable but indicates that the model lacks some dynamics. This is compensated for in Chapter 6 where a new dynamic model for rolling resistance is presented.

5.1 Test Equipment

Three resistance forces mainly affect a vehicle travelling at constant speed on a road: air resistance, rolling resistance and gravitational forces due to slope of the road. Physically they belong to the body of the vehicle, the tires and the mass of the vehicle. With the modular vehicle simulation model created, it is easy to compare simulated results with measurements. For this purpose a heavy truck, a
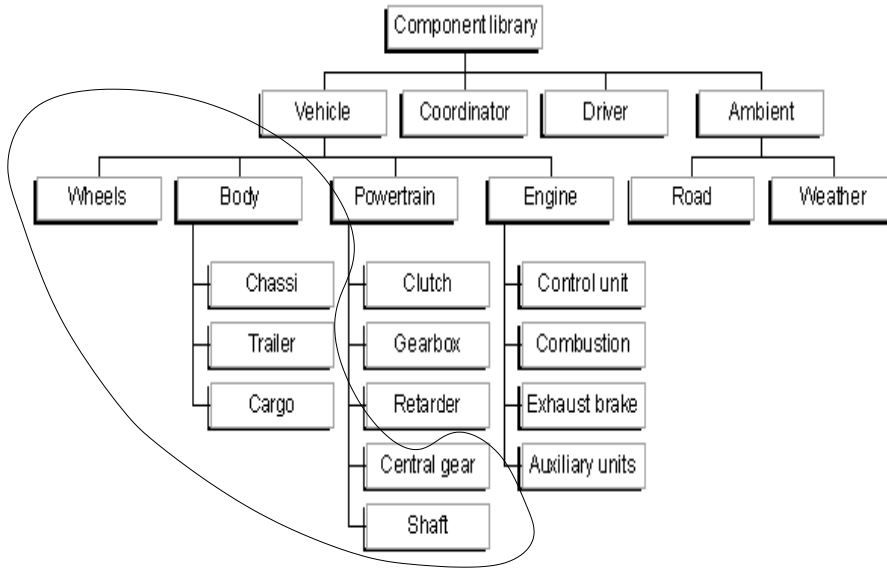
Figure 5.1: Parts of the vehicle model included in the validation of energy
losses. This validation is made possible by use of an extra torque sensor on the
propeller shaft.

SCANIA R124, was equipped with a special propeller shaft. The propeller shaft
was prepared with strain gauges to measure torque and telemetric equipment to
transfer signals from the rotating shaft to the chassis. The equipment is shown
in Figure 5.2.   The vehicle used, seen in Figure 5.3, has earlier been tested in
wind tunnel experiments so the coefficient of air resistance is well known. Values
for the coefficient of rolling resistance for each type of tire used on the vehicle's
different axles were received from the tire manufacturer. The air pressures in
all the tires were controlled according to the manufacturer standards. Before
the test started the weight of the vehicle was carefully measured; the total
weight was 39580 kg. The distribution of weight to the six different axles were
also measured and important distances noted to enable calculation of a correct
center of gravity for the model and thereby ensuring the correct load on each
axle in the model.

    The truck was run until the engine reached normal operating temperature
before any measurements were executed. Since the engine model is based on
steady-state values from test cells, the truck must be driven as near steady state
operation as possible during the validation considered here. The vehicle was
driven on cruise control during all tests in order to keep the speed constant.
All tests were done on Scania's proving ground, where different parts of the
road have defined constant slopes. This ensures a constant load on the vehicle.

Figure 5.2: Strain gauges used to measure true torque on the propeller shaft.

Figure 5.3: Test vehicle used to validate energy losses through measurements of propeller shaft torque.

Together with constant speed this should be sufficient for steady-state operation of the engine.

The testing was done by running the vehicle at constant speeds on a flat road. The vehicle was run at the speeds of; 90, 85, 80, 60 and 40 km/h. This speed range was judged to be appropriate since heavy European trucks are limited to a maximum speed of 85 km/h. Each speed was run four times, two in each direction of the track, resulting in a total number of 20 recordings. The four variables: propeller shaft torque, velocity, engine fueling and engine speed were sampled in 100 Hz.

5.2   Result

In Figure 5.4 the propeller shaft torque at 81 km/h is shown. The oscillations are due to ignitions in the six-cylinder engine. Most recordings are between 8 s and 35 s long. In Figure 5.4 a trend can be seen. The torque on the propeller shaft increases as the vehicle moves over the distance. When travelling in the
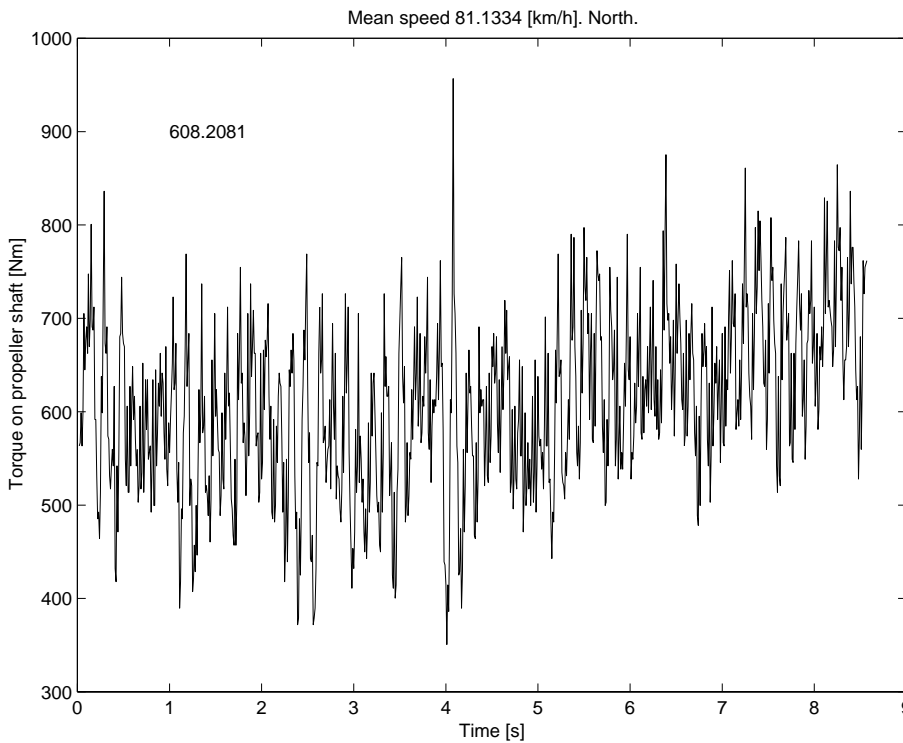
Figure 5.4: Propeller shaft torque at 81 km/h on flat road sampled by 100 Hz. The oscillations are due to ignitions in the six-cylinder engine.

opposite direction it decreases. The same tendency where found on other speeds as well. The road is supposed to be flat (0% slope) but this tells that this was not really true. Fortunately tests were run twice in both directions to eliminate uncertainties like this.

In Figure 5.5, mean values of propeller shaft torque and velocity from all measurements are indicated. As mentioned, four measurements are done on each speed. All of them, except one are then used to form the curve in the figure. One measurement at 60 km/h was extremely short, only three seconds and showed unreasonable high torque and was therefore excluded.
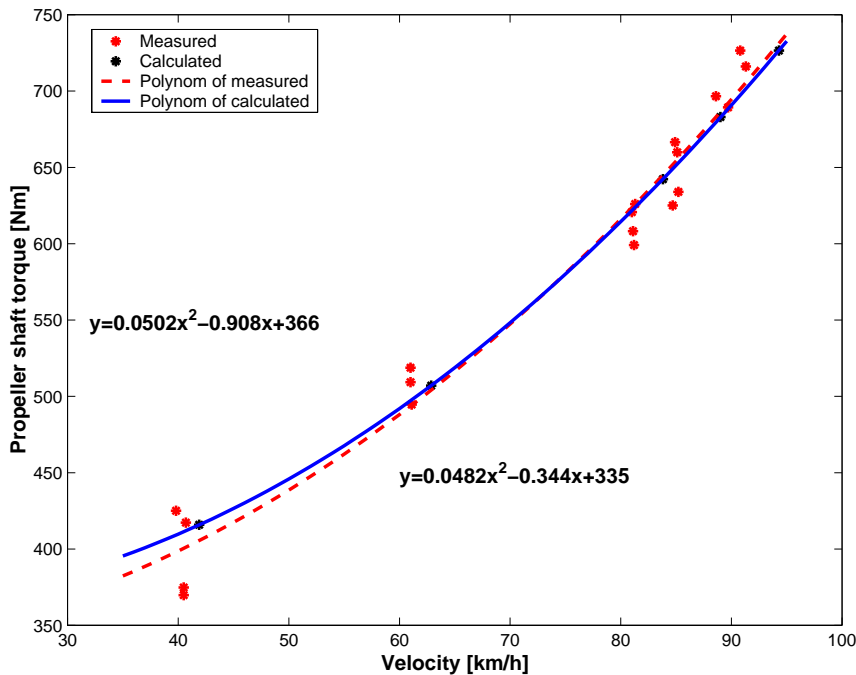
Figure 5.5: Measured and calculated propeller shaft torque at various speeds.

In Figure 5.5 the simulated propeller shaft torques are indicated also. The simulated result (top, dashed line) agrees fairly well with measurements, but is about 3% higher at lower speeds. This is probably caused by the used characteristic for the rolling resistance. According to a tire manufacturer, the coefficient of rolling resistance decrease with increasing speed as seen in Figure 3.17.

The result shown in Figure 5.5 indicates that this is not true for real driving. Both (Wong, 1993) and (H. et al., 1998) states that the coefficient of rolling resistance increases with increasing speed. It is mainly at lower speeds the model differs from the measurements. After discussions with the tire manufacturer it was concluded that the discrepancy probably depends on the way measurements were conducted.

In the beginning of the test high speeds were driven, but the tires were not warm enough giving a too high value of rolling resistance. Then lower speeds were tested but now the tires were warmer than their corresponding steady state temperature, giving a too low value of rolling resistance. The tire manufacturer claims it takes one hour of driving at constant speed to reach steady state temperature in the tires. This does not illustrate practical driving. The conducted test can be said to illustrate highway driving followed by a shorter distance with lower speed (passing though a town), in which case the tires will be too hot.

This gives an indication that there is a need for a more dynamic model for the coefficient of rolling resistance to compensate for tire temperature.

5.3   Validation

Due to the modular design and the non-causality used in the modeling language it is possible to validate parts of the vehicle model separately. The model is shown in Figure 5.6, where a block of constant acceleration equal to zero is inserted on the propeller shaft to obtain steady state. This also illustrates the strength of the non-casual modeling. The computational causality of this model is inverted compared to the one in Figure 4.2.

By using of the interface between Dymola and Matlab, an optimization problem can be formulated in Matlab to find the set of parameters that minimize the difference between the measurements and the model. Scaling factors were introduced for the constants a and b in the expression for the coefficient of rolling resistance (Equation (3.13)), for the losses in the wheel bearings, and for the air resistance. For the rolling resistance this means that the expression for C_r is changed but the level at 80 km/h is kept according to the ISO standard (recall Section 3.4.2).

One common problem in object-oriented modeling is that the model gets over-parameterized meaning that there are several parameters affecting one phenomenon. One example is here the propeller shaft torque. It is affected by the air resistance and the rolling resistance which both are dependent on the speed in square, Equation (3.5) and Equation (3.13). This means that there are two parameters in the model that can be tuned to get a good agreement with measurements. Since the vehicle has been tested in wind tunnel it is concluded that the largest uncertainty is in the tires.

The optimization mainly resulted in a new expression for the coefficient of rolling resistance. The result is shown in Figure 5.7 as the solid line. The air resistance was adjusted up 0.5% and the losses in the wheel bearings were adjusted up 7%. This gave a good agreement with the measurements. The difference is now less than 0.015 Nm at all speeds. Nevertheless, even though the overall match is good, the parameter adjustments that were necessary to get agrement are of such a size and structure that they indicate that there is a mismatch between data and model structure.
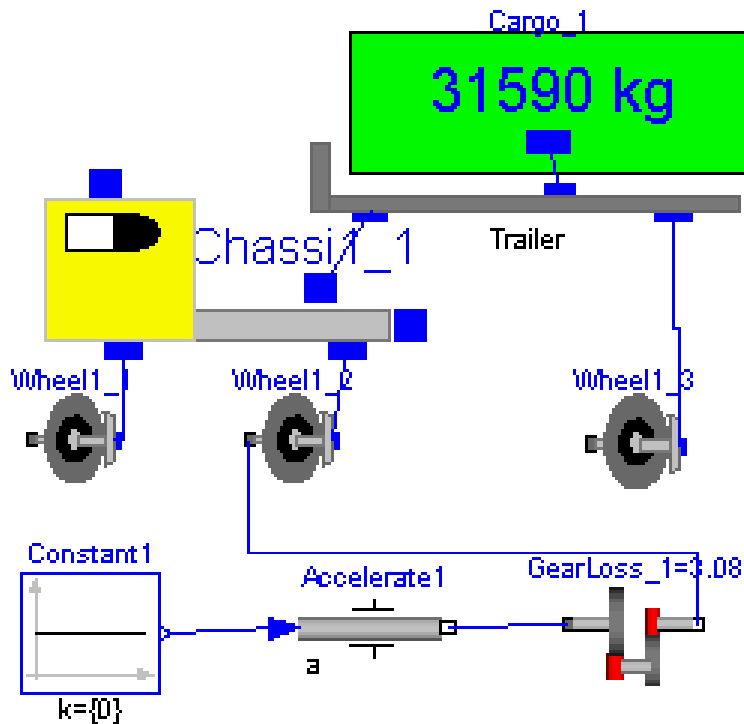
Figure 5.6: Model used for validation of propeller shaft torque.

5.4   Comments

The experiments presented in this chapter are all conducted on a flat road at various constant speeds. Other less successful experiments were conducted as well. One attempt was to measure the propeller shaft torque while driving up a hill with constant slope. Due to the large torque required in the hill the wheel suspension forces a movement between the axle and chassis. This movement introduced a shortcut in the telemetric system used.

Coast down tests are widely used for passenger cars to determine air resistance and rolling resistance. This was also tried with this truck mainly to see if it was possible to identify the rotating inertias in the powertrain. It was found to be hard since the large weight of trucks gives very long retardation times. To coast from 90 km/h to 30 km/h takes about 250 seconds with a 40000 kg truck. This require a very long distance with constant slope which is hard to find. Another problem with this approach is, like described above, that the coefficient of rolling resistance varies with tire temperature. From Figure 5.7 it is also clear that the actual C_r (solid) differs from the steady state values (dashed). The conclusion is that some slow dynamics is involved.
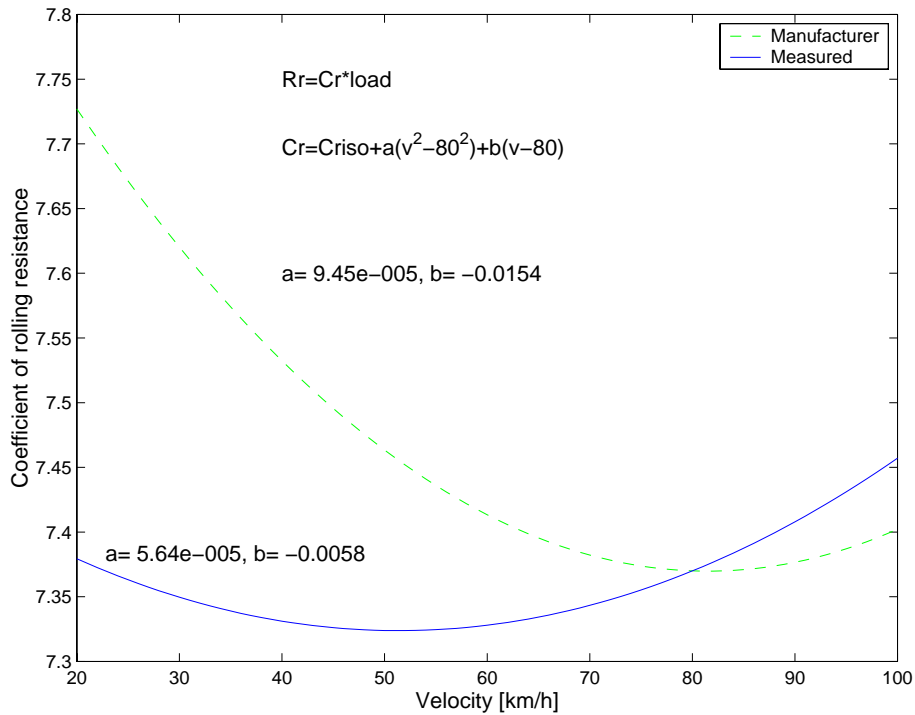
Figure 5.7: New (solid) and old (dotted) expression for the coefficient of rolling resistance

5.5   Conclusions

Experiments with a heavy truck equipped with strain gauges to measure torque on the propeller shaft are conducted to validate the forces of air resistance and rolling resistance in the model. It is found that an expression for rolling resistance as a function of vehicle speed only is to simplistic to obtain a good match.

The major contribution of this experiment is that rolling resistance for truck tires is strongly dependent on tire temperature and that the time constant for rolling resistance and tire temperature is long. These facts are investigated further in Chapter 6.

It is also found that the non causal modeling that Dymola provides is very powerful in validation and optimization. The vehicle model is fitted to the measured data with good accuracy.

<div align="right">

6

</div>

New Model for Rolling Resistance

As seen in the previous chapter it turned out that the obtained data did not match completely with a traditional model of rolling resistance. Modifications had to be made on the expressions for air resistance and wheel bearing losses as well. The experiments indicate that there are dynamics involved (interpretation of Figure 5.7). In this chapter one single dynamic effect, tire temperature, will be added resulting in a new model for rolling resistance. The new model relates rolling resistance to tire temperature and speed. It can explain the result from Chapter 5 and is in good agrement with results published by others.

6.1   Introduction

In Chapter 3.4.2 on page 36, R_r and C_r were defined as the rolling resistance force and the coefficient of rolling resistance. There, many factors influencing them were also presented.Most of these factors do not change during normal driving and can therefore be neglected in this type of simulations. As shown in the previous chapter the rolling resistance is also strongly dependent on the temperature of the tire. This chapter therefore presents a model where C_r mainly depends on tire temperature, T, and speed, v, so that

$$C_r = C_r(T, v) \tag{6.1}$$

The temperature has a large effect known to affect C_r by 100% or more. See for example Figure 6.1 which is obtained from (Wong, 1993). It is a slow effect with time-constants for truck tires up to 30 minutes (Popov et al., 1999). Tires for passenger cars usually has time-constants around 10 minutes.

<div align="center">

63

</div>
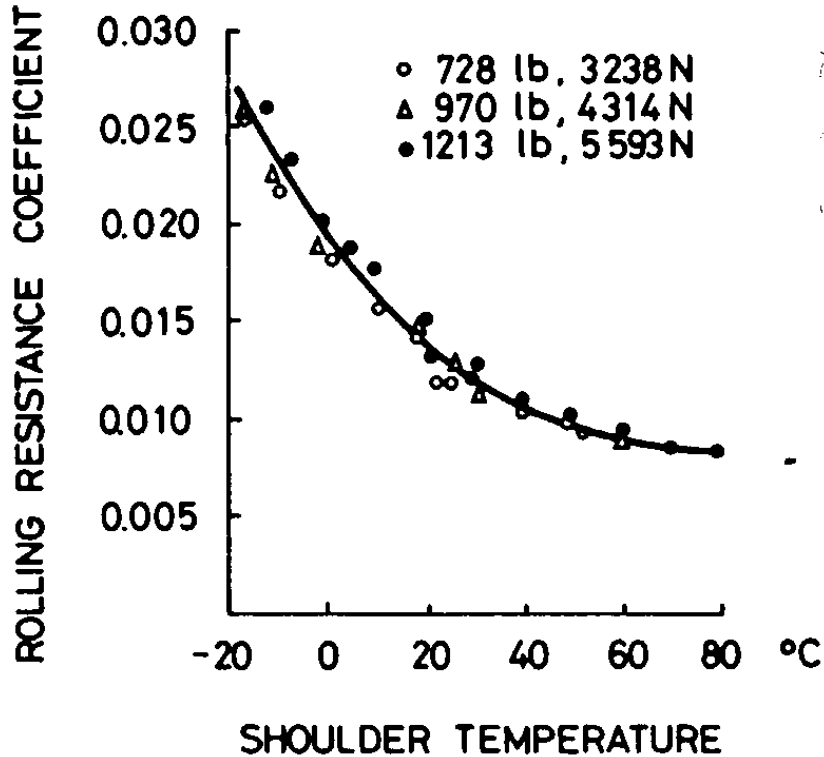
Figure 6.1: Variation of rolling resistance coefficient with tire shoulder temperature. The figure is obtained from (Wong, 1993)

A natural cause for the strong relation between rolling resistance and tire temperature is the effect tire temperature has on the inflated air pressure. When the tire gets warmer, the air pressure increases and the rolling resistance decreases. This is illustrated in (Popov et al., 1999). The heating of the tire, and thus the temperature depends on the velocity, v, but also on ambient conditions.

The rolling resistance is known to depend also on the velocity even if the temperature or, almost equivalently, if pressure is constant. This is obtained from experiments where the tire is kept at rated pressure (Bauer, 1996; Wong, 1993) expressions like

$$\tilde{C}_r = \tilde{C}_{r0} + \tilde{C}_{r1}v^2 \tag{6.2}$$

are obtained. The effect of the speed is smaller than the temperature effect but still significant. The variation, i.e. the term $\tilde{C}_{r1}v^2$, may be 20-30% compared to $\tilde{C}_{r0}$ (Wong, 1993).

6.2 Stationary Conditions

First, it is important to observe that the concept of stationary conditions has different definitions in the classical papers, since different variables have been held constant during experiments. For example, in (van Eldik Thieme, 1971) the inflation pressure and vertical load has been held constant at the rated value, which means that pressure adjustments must be made during experiments when the tire warms up. Others keep the inflation pressure and tire deformation (height of axle) constant (Lippman et al., 1978). To test tires like they are used in vehicles the inflation pressure should be adjusted before start of test and the vertical load be kept constant as in (Popov et al., 1999; Janssen and Hall, 1980). The definition used here is based on real driving with a vehicle.

Definition 2. *Stationary conditions are obtained after driving a vehicle straight ahead at constant speed on a flat road for a sufficiently long time to obtain constant conditions.*

Vehicle Velocity

The basic variable in the definition of stationary condition above is the vehicle velocity, v.

Tire Temperature

Different parts of the wheel will have different temperatures, but it has been shown that the tire shoulder temperature and the inflated air has about the same temperature at stationarity (Janssen and Hall, 1980). It is here defined as the tire temperature at stationary conditions, T_{sc}.

This temperature is of course a function of several variables like for instance vehicle speed and ambient temperature $T_{sc} = g_{sc}(v; T_{amb}, ...)$. Nevertheless, for a specific driving scenario, the stationary temperature T_{sc} will mainly be a function of v only i.e.

$$T_{sc} = g_{sc}(v) \tag{6.3}$$

Coefficient of Rolling Resistance

The coefficient of rolling resistance at stationary conditions will be denoted C_r^{sc}. Also the rolling resistance is a function of other variables like ambient temperature etc, $C_r^{sc} = C_r^{sc}(v; T_{amb}, ..)$. With the same argument as in the case of tire temperature, C_r^{sc} is mainly a function of velocity, v, i.e.

$$C_r^{sc} = C_r^{sc}(v) \tag{6.4}$$

6.2.1 Measuring $C_r^{sc}(v)$

The values of the rolling resistance coefficient can be directly obtained by measurements according to Definition 2. The vehicle is driven at constant speed

until stationary conditions are obtained, which typically would be considered
to occur after one or two hours.

This will result in values that according to previous experience and to oral
information from tire manufacturers can be described by a second order poly-
nomial

$$C_r^{sc}(v) = a_0 + a_1 v + a_2 v^2 \qquad (6.5)$$

The values of a_0, a_1, a_2 will result in different shapes of $C_r^{sc}(v)$ where Figure 6.2
gives two alternatives. Both curves have the expected characteristics of de-
creasing values to start with. This is due to temperature effects influencing
inflated air pressure. The left curve is dominated by the temperature effect and
is monotonically decreasing. It shows the same characteristics as Figure 6.1.
The right curve in Figure 6.2 is decreasing for lower speeds, but then reaches
a turning point where C_r^{sc} starts to increase with increasing speed. The speed
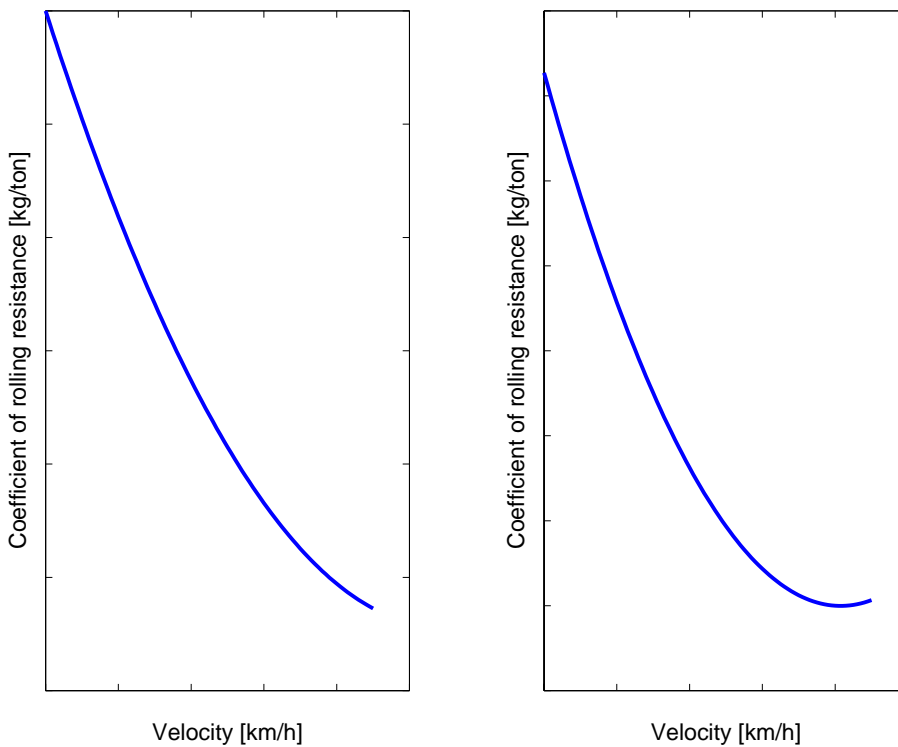
Figure 6.2: Two alternatives for the coefficient of rolling resistance as function
of vehicle speed at stationarity.

for which this turning point of minimum C_r^{sc} occurs, whether or not it occurs
within the operational range of speeds, of course depends on tire construction

and tire properties. It seems that for modern truck tires, the turning point with minimum C_r^{sc} occurs somewhere in an interval around 80 km/h.

Throughout the rest of the chapter the version to the right in Figure 6.2 will be used for illustration, since this characteristics has been observed in our measurements and also is in accordance with the results obtained from the tire manufacturer Michelin.

6.2.2   Relating $C_r^{sc}(v)$ to Temperature

The rolling resistance at stationary conditions was obtained as a function of velocity, v. Notice also that a given velocity results in a certain temperature of the tire, T_{sc}, described by Equation (6.3) as $T_{sc} = g_{sc}(v)$. This can be used to define the stationary rolling resistance coefficient as a function of temperature. Introduce $C_{r0}(T)$, valid not only for stationary conditions, but defined so that it coincides with C_r^{sc} for stationary conditions

$$C_{r0}(T) = C_{r0}(g_{sc}(v)) = C_r^{sc}(v) \qquad (6.6)$$

This simply defines $C_{r0}(T)$ by a scaling of the x-axis by $T = g_{sc}(v)$, as illustrated in Figure 6.3. This figure also illustrates the relation between v and T_{sc}.
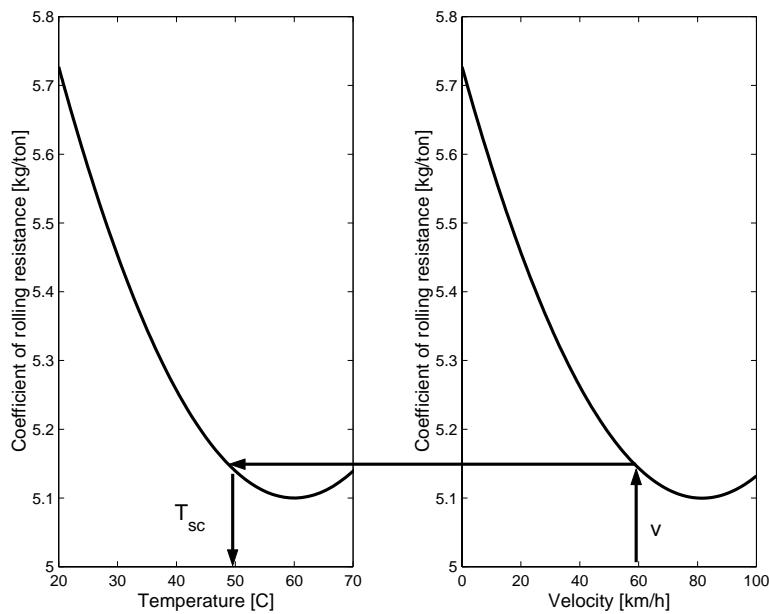
Figure 6.3: Coefficient of rolling resistance, illustrating the relation between v and T_{sc} at stationarity.

6.2.3 Inverting g_{sc}

The velocity corresponding to a given temperature, assuming stationary conditions, will be needed later. Denote this velocity v_{sc}. This is easily obtained by using the inverse function of g_{sc} defined in Equation (6.3). The function g_{sc} is monotonous in v.

$$v_{sc} = g_{sc}^{-1}(T) \tag{6.7}$$

6.3 Velocity Transients

The stationary behavior will now be complemented with transient velocity behavior. Consider a change in velocity that is so fast that the thermodynamic properties of the tire does not change. (The change needs not to be especially fast since the temperature time-constant is up to 30 min). The behavior of C_r is then described by a relation like Equation (6.2), but the level depends on where it is on the stationary condition curve. This is illustrated in Figure 6.4 where the dashed curve shows the coefficient of rolling resistance for stationary conditions. Consider a vehicle driven at 35 km/h long enough to reach the stationary level. If the speed now is changed quickly the rolling resistance will change according to the solid line since the temperature of the tire has not changed yet.

6.4 Model of Rolling Resistance Coefficient

The model of the coefficient of rolling resistance is now obtained by combining Equation (6.2) and Equation (6.6). This gives

$$
\begin{aligned}
C_r(T, v) &= C_{r0}(T) + C_{r1} \cdot (v^2 - v_{sc}^2) \tag{6.8} \\
v_{sc} &= g_{sc}^{-1}(T) \tag{6.9}
\end{aligned}
$$

The model is thus a combination of the steady-state behavior $C_{r0}(T)$ and a velocity term (compensated by v_{sc} so that the correct stationary value for C_r is obtained when $v = v_{sc}$).

6.4.1 Remark

For a fixed temperature, being the case for short transients, the model in Equation (6.8) has the same structure as the classical model, Equation (6.2), with dependence on v^2. However, the parameterization is slightly different and the relation between the two parameterizations is described by

$$
\begin{aligned}
\tilde{C}_{r0} &= C_{r0}(T) - C_{r1} \cdot (g_{sc}^{-1}(T))^2 \tag{6.10} \\
\tilde{C}_{r1} &= C_{r1} \tag{6.11}
\end{aligned}
$$

The second equation implies use of $\tilde{C}_{r1} = C_{r1}$ i.e. measured values from traditional velocity experiments can directly be used, which is an advantage.
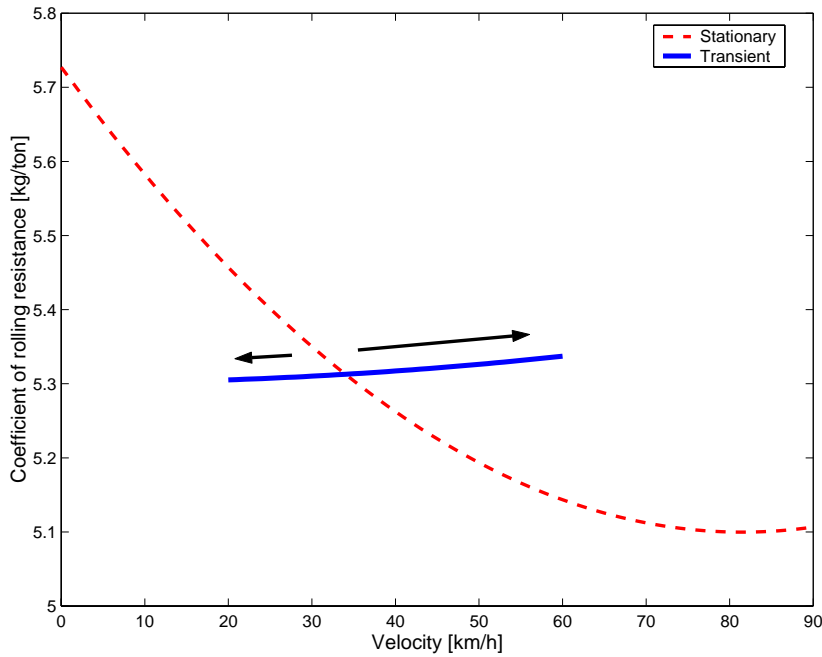
Figure 6.4: A tire at stationary conditions at 35 km/h will for a quick velocity transient follow the solid line for the coefficient of rolling resistance. The dashed line is only valid for stationary conditions.

6.5 Thermodynamic Tire Behavior

A detailed description of tire thermodynamics is of course complicated, since many parts of the wheel are involved creating complex heat generation and heat transfer. For each part of the wheel (tire shoulder, inflated air, rim,..) an energy equation can be formed of the type

$$mc\frac{dT_i}{dt} = q_{in}(T_i, ..., T_n) - q_{out}(T_1, ..., T_n) \quad i = 1, ..., n \qquad (6.12)$$

Where m is the mass of the part, c is the specific heat capacity of the part, T is the temperature of the part and q_{in}, q_{out} are the energy generation/inflow in/to the part and energy outflow from the part.

The important point now is that this complicated system of energy equations can be vastly simplified but still able to capture the behavior that is important for rolling resistance. The first observation is that two important temperatures, the shoulder temperature and the temperature of the inflated air, are about the same as shown in (Janssen and Hall, 1980). This temperature is denoted by T. Next, the energy outflow is with reasonable accuracy proportional to the

temperature T i.e.

$$q_{out} = \beta T \tag{6.13}$$

This is a standard assumption, but here it is further motivated by the fact that it leads to exponential time responses which has been demonstrated to be the case by (Popov et al., 1999). Introducing Equation (6.13) into Equation (6.12) result in an energy equation of the form

$$\frac{dT}{dt} = -\frac{\beta}{mc}T + \frac{1}{mc}q_{in} \tag{6.14}$$

Introduce the time constant τ as

$$\tau = \frac{mc}{\beta} \tag{6.15}$$

Introducing Equation (6.15) into Equation (6.14) leads to

$$\frac{dT}{dt} = -\frac{1}{\tau}(T - \frac{1}{\beta}q_{in}) \tag{6.16}$$

Finally, the term $\frac{1}{\beta}q_{in}$ describing energy generation in the tire is of course also very complex. However, the main heat source comes from tire deformation work which is velocity dependent. This fact together with the model of stationary conditions in Section 6.2 lead to a model in the following way.

At stationary conditions Equation (6.3) holds and the temperature is not changing, $\frac{dT}{dt} = 0$, which written out is

$$\frac{dT}{dt} \quad = \quad 0 \tag{6.17}$$

$$T = T_{sc} \quad = \quad g_{sc}(v) \tag{6.18}$$

Introducing these into Equation (6.16) gives

$$0 = -\frac{1}{\tau}(T_{sc} - \frac{1}{\beta}q_{in}) \tag{6.19}$$

which leads to

$$\frac{1}{\beta}q_{in} = T_{sc} = g_{sc}(v) \tag{6.20}$$

Equation (6.20) now describe the energy generation term $\frac{1}{\beta}q_{in}$ that is difficult to model directly. It is described in terms of stationary temperature, T_{sc}, which is readily obtained from measurements at stationary conditions. Introducing Equation (6.20) back into Equation (6.16) leads to the final model

$$\frac{dT}{dt} \quad = \quad -\frac{1}{\tau}(T - T_{sc}) \tag{6.21}$$

$$T_{sc} \quad = \quad g_{sc}(v) \tag{6.22}$$

where T_{sc} is obtained from stationary conditions and τ can be measured (or estimated) like in (Popov et al., 1999).

6.6 Complete Model

The complete model is obtained by combining the rolling resistance, Equations (3.11), (6.8), and (6.9), with the thermodynamic model of the tire, Equations (6.21) and (6.22). Collecting the equations leads to

$$
\begin{aligned}
R_r &= C_r(T, v) \cdot N \\
C_r(T, v) &= C_{r0}(T) + C_{r1} \cdot (v^2 - v_{sc}^2) \\
v_{sc} &= g_{sc}^{-1}(T) \\
\frac{dT}{dt} &= -\frac{1}{\tau}(T - T_{sc}) \\
T_{sc} &= g_{sc}(v)
\end{aligned}
$$

The final model is based on sound physical principles. It is explicitly dependent on the two physical variables that are important for rolling resistance, namely tire temperature, T, and velocity, v. The model contains two parameters, C_{r1} and τ, and a steady-state curve, g_{sc}. The measurement and/or estimation of them follow sound and simple procedures well related to classical results.

6.7 Behavior in $C_r - v$-diagram

As argued above, the coefficient of rolling resistance, C_r, is not a pure function of velocity, v. Still, it may be informative to plot the behavior in a $C_r - v$-diagram. The stationary curve is illustrated as a dashed line in Figure 6.5 and Figure 6.6.

6.7.1 Change of Speed

First consider a situation where the vehicle has been driven at 80 km/h so long that stationary conditions have been obtained which corresponds to point 1 in Figure 6.5. The vehicle then decreases its speed to 50 km/h for example due to a speed limit. This transition is fast (a handful of seconds or at least clearly less than a minute) so it will result in a transition to point 2 in Figure 6.5. The transition is here described by Equation (6.8). At this point the tires are hotter than their stationary temperature at 50 km/h resulting in a lower value of rolling resistance. The vehicle is then driven in 50 km/h for a long time and the tires are cooled off. This will cause a transition from 2 to 3 that will take in the order of one or two hours.

6.7.2 Intermittent Change of Speed

Consider now a driving scenario where the vehicle is driven at 80 km/h passes a town and drives 50 km/h for 15 minutes, and then goes back to 80 km/h. This will result in an $C_r - v$-diagram as in Figure 6.6. During the 15 minutes at
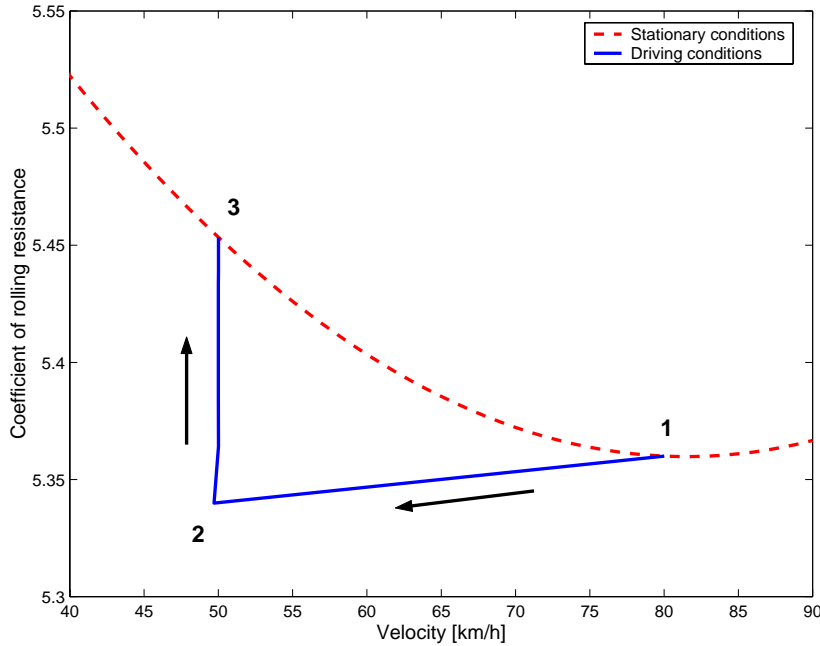
Figure 6.5: Stationary conditions at 80 km/h followed by a longer period of 50 km/h gives this path to the stationary level of rolling resistance at 50 km/h.

50 km/h the tires are cooled off, resulting in a higher value of rolling resistance (point 2 to point 3). When the speed is increased again it results in the transition point 3 to point 4. Then the tires will be warmed up and reach the stationary value of rolling resistance at 80 km/h (point 1).

6.8   Verifying Experiments

As seen in Chapter 5 it was impossible to fit a model to the measured data only by using a speed dependent coefficient of rolling resistance. Modifications had to be made to air resistance and wheel bearing losses as well.

In Figure 5.5, it was seen that the measured propeller shaft torque was 3% lower then simulated torque at lower speeds. The difference was assumed to depend on the stationary model for rolling resistance used without knowledge of the effect of tire temperature. To see if the new dynamic model for rolling resistance can improve the situation it was implemented in a vehicle model like in Figure 4.2. The whole test was then simulated including warm up and periods at different constant speeds.

The test cycle is shown in Figure 6.7. It starts with a warm up period at 80 km/h for 15 minutes. It is followed by periods at 90, 85, 80, 60 and 40 km/h.
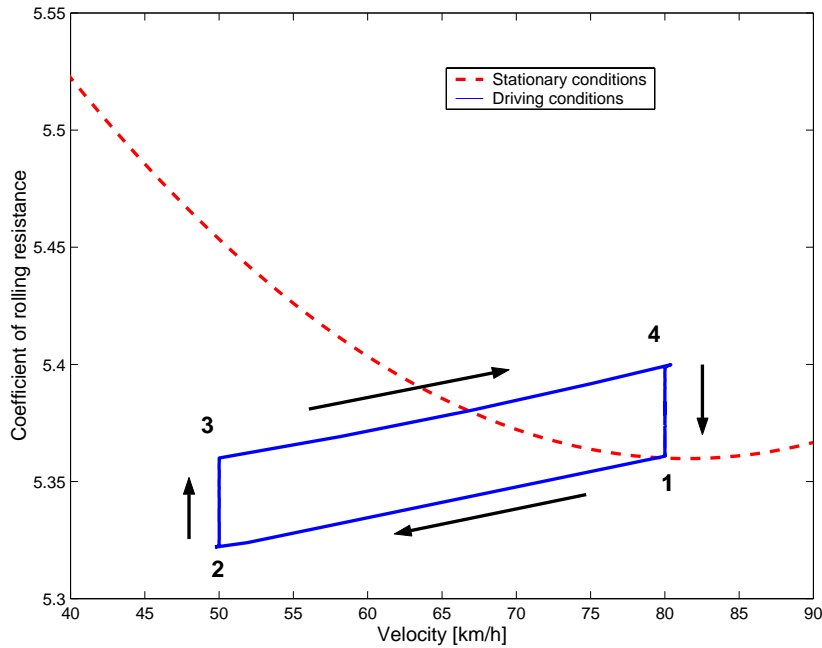
Figure 6.6: Stationary conditions at 80 km/h followed by a shorter period of 50 km/h and then 80 km/h again causes this change in rolling resistance due to changes in tire temperature.

In the figure the tire temperature (dashed) calculated by the proposed model is shown also, starting at 40 °C. It can be seen that the tires reach their maximum temperature after 2300 seconds (38 minutes) at the end of the period of 80 km/h.

As the tire temperature changes, so does the coefficient of rolling resistance and the need for torque on the propeller shaft. In Figure 6.8 the measured and simulated torque are compared. The measured values are the same as in Chapter 5 and in the simulations the new model from this chapter has been used. It is hard to see any difference. Observe that this superior result was obtained without artificially releasing other model parameters as was done in the earlier optimization.

In Figure 6.9 the resulting coefficient of rolling resistance is shown. It can be seen that the proposed model for rolling resistance directly gives the same type of curve as earlier was achieved through optimization, shown in Figure 5.7. The model thus captures the difference between static and dynamic rolling resistance. Compared to Figure 5.7 there is a differing offset. This offset was compensated by the optimization through increased losses in the wheel bearings. This is not needed anymore using the new model.
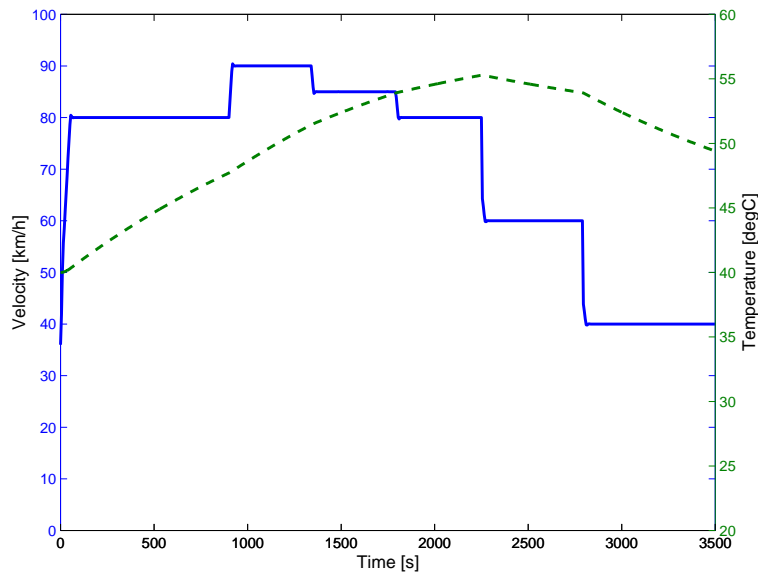
Figure 6.7: Description of test cycle. Velocity - solid line; estimated tire temperature - dashed line.
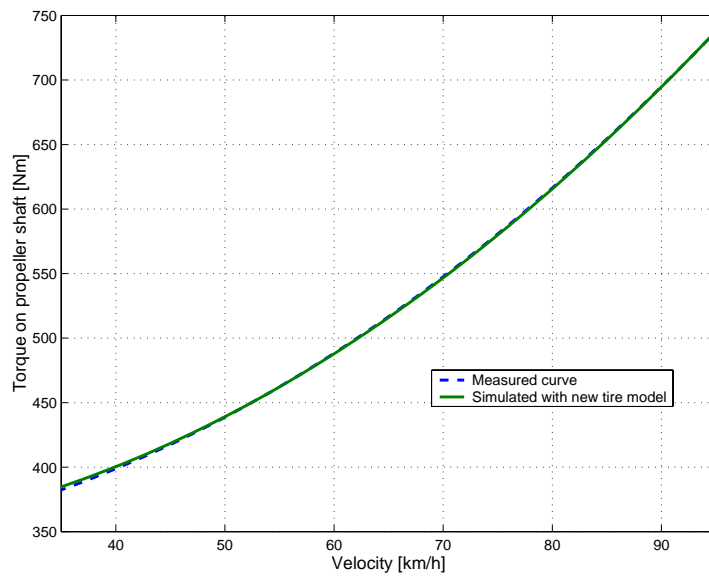
Figure 6.8: Measured and simulated propeller shaft torque at various speeds. In the simulations the proposed model for rolling resistance has been used.
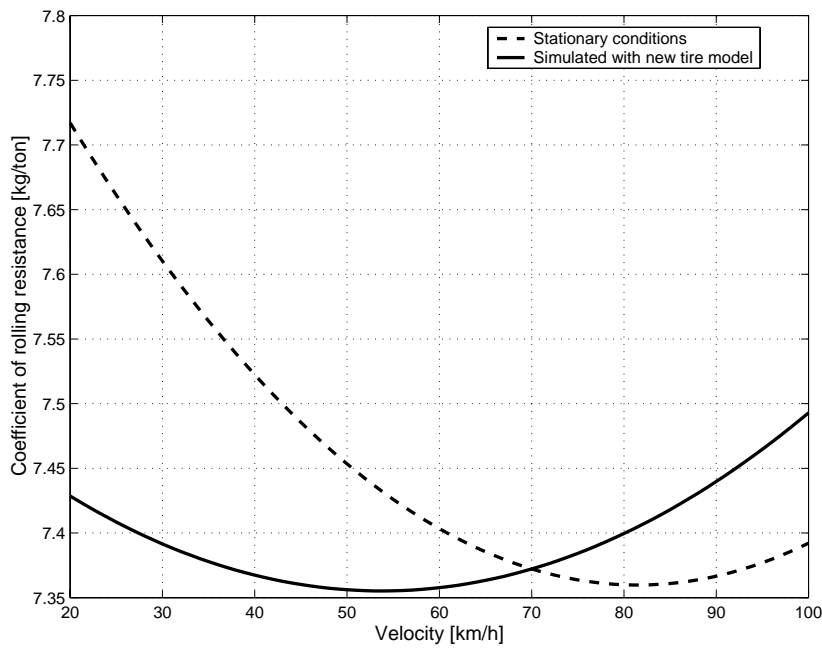
Figure 6.9: Coefficient of rolling resistance. Simulated with proposed model - solid line. Values at stationary conditions - dashed line. Characteristics similar to the curves in Figure 5.7 are obtained directly from the new model without the need for any extra fitting or optimization.

6.9 Conclusions

A new model for rolling resistance of pneumatic tires is presented. It is based on known properties of tires and own observations. The model states that the coefficient of rolling resistance is a function of tire temperature and vehicle speed. It consists of a differential equation for the tire temperature and and a relation between velocity and stationary temperature. In this way both fast and slow phenomena can be described.

The new model is in good agreement with results published by others. Further, in own experiments with a heavy truck the new model show a very good ability to calculate the true dynamic rolling resistance.

7

Validation of Fuel Consumption

To be able to predict fuel consumption for heavy trucks, more than propeller shaft torque must be validated. This chapter is a natural continuation of the validation in Chapters 5 and 6. Here the rest of the vehicle model, gearbox, retarder, engine, road and weather are validated. The emphases is on the engine model and on the road model including altitude measurements and calculations of the slope of the road. This is illustrated graphically in Figure 7.1.

The purpose with this chapter is to validate fuel consumption for a truck in highway driving. The method used is to drive the vehicle a certain distance, measuring topography and actual speed, and at the same time measuring fuel consumption. A simulation with an identical vehicle, using the measured road profile as input, is used to compare signals and fuel consumption.

The chapter starts with presenting the test procedure and equipment. The preparations include wind tunnel experiments for the vehicle and testing of the engine in test cell. Section 7.2 presents results from three measurements with the test truck on the highway. Measured speed and distance are found to be difficult to measure correctly since they are influenced by axle load and tire slip. Two methods for measuring fuel consumption are compared: using signals from the engine control unit or using cans. Section 7.3 starts with a sensitivity analysis to see which parameters effects fuel consumption most. One important parameter is slope of the road. However, slope is not measured so it must be obtained through derivation, followed by filtering to get realistic smoothness of the road.A good agrement in these areas together with the results from Chapters 5 and 6 should also mean a good level of accuracy in fuel consumption. This comparison is done last in Section 7.3.
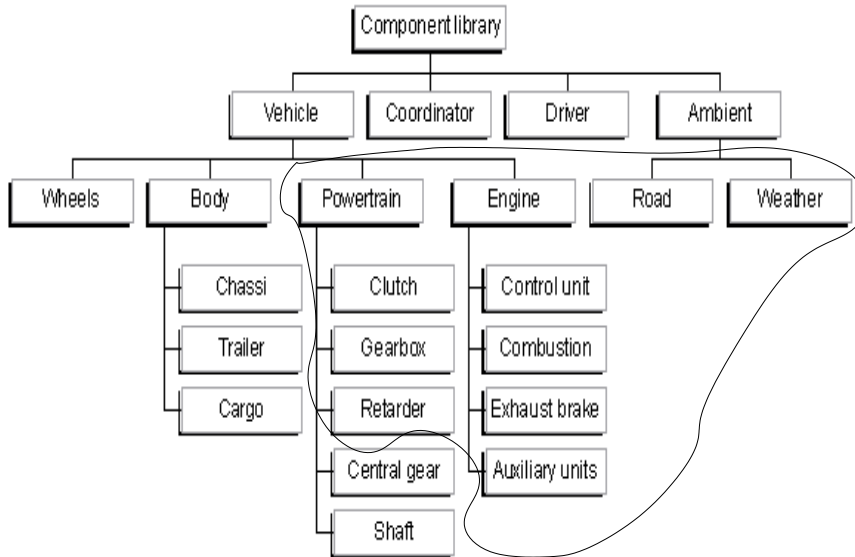
Figure 7.1: All parts of the vehicle model are included in the validation for fuel consumption. The emphases is on the parts within the circle, the others are validated in Chapter 5.

7.1   Test Procedure and Equipment

This section describes the procedure to measure fuel consumption and the type of test equipment used. The test equipment are divided into different areas dependent on their purpose: fuel measurement, vehicle, engine, road distance, road altitude.

7.1.1   Fuel Measurement

To achieve a good accuracy in fuel consumption measurements the test truck was equipped with a specially designed fuel tank avoiding air slots in the tank during fill up. It had a high filling pipe connected with pipes that evacuates air bubbles caused by possible road inclination at the filling station.

The procedure to measure fuel consumption was:

1. Fill the tanks up with fuel.

2. Drive the test road.

3. Refill and measure the consumed mass of fuel.

The accuracy of the filling station is 0.5% and was not judged to be accurate enough. Instead cans were used to fill up the tank. The weight of them were controlled empty, full with diesel and after filling up the truck. By use of the mass density for the fuel, the volume of the consumed fuel could then be calculated. The accuracy of the scale was ± 10 g and an average filling was 64 kg which gives a total accuracy of 0.015%. The mass density of the fuel was determined by a laboratory to 814 g/dm^3.

The engine was controlled by a special control unit allowing connection to a PC. In this way internal signals from the control unit can be measured at 100 Hz. The measured signals are displayed in Table 7.1. By integration of the flow of fuel, like described in Equation((3.6)-(3.8)), the consumed volume of fuel is calculated. This is the same way fuel consumption is calculated in the simulations.

Vehicle speed	[km/h]
Engine speed	[rpm]
Fueling	[mg/stroke]
Boost pressure	[mbar]

Table 7.1: Control unit variables measured with 100 Hz.

7.1.2 Vehicle

A heavy truck, identical to the one seen in Figure 5.3, was used during these tests. The truck had a 12 liter diesel engine and a 12 speed gearbox that was operated manually. Wind tunnel tests had earlier been done with an identical vehicle so the coefficient of air resistance was fairly well known. Tire data, like effective radius, R_e, and coefficient of rolling resistance, C_r, were received from the tire manufacturer for each type of tire used on the vehicles five different axles. The air pressures in all the tires were controlled according to the manufacturer standards. Tire data are summarized in Table 7.2. This means that

	Tire Dimension	Tire Tread	Measured pressure [bar]	R_e [m]	C_r [1/1000]
Front axle	315/80R22.5	XZA E	6.5	0.520	4.70
Drive axle	315/80R22.5	XDA E	5.3	0.522	5.36
Trailer axles	385/65R22.5	XTA E	7.8	0.496	4.5

Table 7.2: Tire data for the test vehicle.

the validation from Chapter 5 can be used and only values of tire parameters like radius and coefficient of rolling resistance need to be changed. In Table 7.3 the weight distribution of the vehicle is shown. These data are used to calculate the two centers of gravity, of the truck and of the trailer. The total weight was 39360 kg.

	Weight [kg]
Truck only, front axle	5300
Truck only, drive axle	2040
Whole vehicle, front axle	6720
Whole vehicle, drive axle	9240
Whole vehicle, 3rd axle	7800
Whole vehicle, 4th axle	7800
Whole vehicle, 5th axle	7800
Whole vehicle, total	39360

Table 7.3: Weight distribution for the test vehicle used to calculate the two centers of gravity.

7.1.3   Engine

To eliminate the uncertainty of the engine individual, one engine was first tested in an engine test-cell with the same type of fuel that is used on roads. Thereafter this engine was mounted in the test truck. Results from the test cell are shown in Figure 7.2. This specific engine gave a maximum output of 401 hp, even though the nominal power of this type of engine is 420 hp. The difference depends mainly on the used fuel quantity since it has a lower energy density than nominal. The data from the test cell is used by the simulation model in the comparison with real measurements from the road.
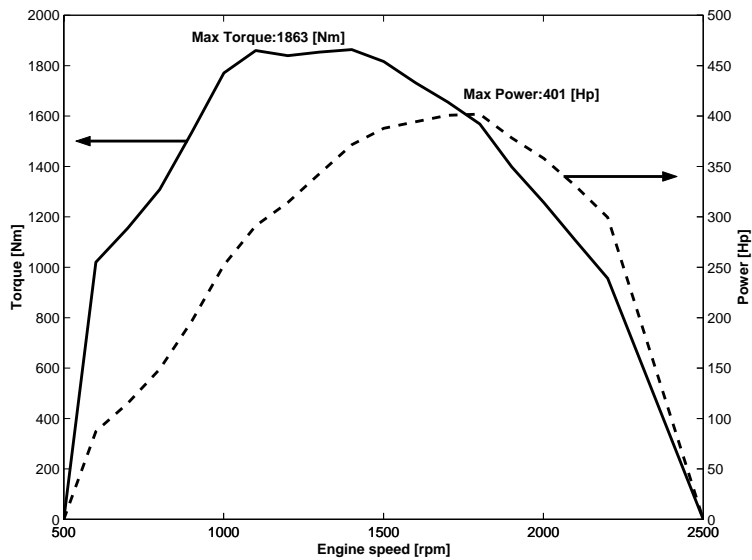
Figure 7.2: Maximum engine torque and power for the used engine.

7.1.4 Road Distance

A good way to measure speed and distance is to use a "5th wheel" shown in Figure 7.3, which is a bicycle wheel with speed sensor. Since this wheel is so light and is not affected by any torque, the slip of the wheel becomes very low and this enables good accuracy in speed and distance measurements. The wheel is towed behind the vehicle mounted on a joint allowing it to well follow the vehicle in turns and over irregularities in the road.

Figure 7.3: 5th wheel mounted after the truck to measure speed and distance.

Unfortunately the 5th wheel could not be mounted on the test truck at the same time as the trailer since there was too little space between the truck and the trailer. The distance of test road was therefore measured at an additional occasion using the 5th wheel on the truck without trailer. The result is compared with signals from the vehicle.

7.1.5 Road Altitude

To record the profile of the actual road, Scania has a portable equipment that records the altitude, actual speed and actual distance. A typical profile of a road recorded with this equipment has previously been shown in Figure 3.23.

The equipment uses the fact that the ambient air pressure is related to the altitude, by using a barometer to measure the air pressure and calculate the altitude. The speed and distance signals are taken from the vehicle. Speed and altitude are stored three times per second. This is a flexible equipment that can be used in any vehicle in any part of the world. The disadvantages are that it is sensitive for weather changes and that it is necessary to keep all windows of the vehicle closed and the fan in the cabin at constant speed.

7.2   Results

This section presents results from the three measurements of fuel consumption. The quality of the measured signals is also studied and discussed. The signals are distance, road altitude, vehicle speed, engine boost pressure and total fuel consumption.

The road between Södertälje and Norrköping was used for the fuel consumption tests. It is a fairly flat freeway which is 122 km one way. The return trip though starts with a rather steep uphill climb. This distance was run at three different occasions with almost the same ambient conditions. Ambient air pressures and temperatures before start are shown in Table 7.4 for the three tests. The main part of the distance the truck was run with the cruise control on, set to 85 km/h. Downhill, the constant speed control of the hydraulic retarder was activated at 90 km/h.

	Air temperature [Celcius]	Air pressure [hPa]
Day 1	10.3	992
Day 2	8.6	1001
Day 3	6.0	1005

Table 7.4: Ambient conditions at the test days.

7.2.1   Road Distance

Regulations demand that speed and traveled distance displayed for the driver are measured on the driving axle. Heavy trucks are rear wheel driven and the speed is measured on the outgoing axle of the gearbox. A problem with this is that the load on the rear axle can vary much on a truck, between 2000 kg to 10000 kg as seen in Table 7.3. This influences the deflection of the tires and their effective radius strongly, and therefore the difference between real and indicated speed show variations with rear axle load. Additionally, driving torque disturbs this difference even further by introducing slip which means that the effective radius decreases. An example of these variations can be seen in Table 7.5, where the distance for the test road measured with the 5th wheel is compared with the vehicle instruments with and without trailer (axle load). As seen the instruments in the truck always shows a too long distance, 1.4% with trailer and 0.8% without. The change is due to the difference in axle load. With trailer the truck showed exactly the same value all three times. The error with trailer is of the same magnitude as slip is expected to be. A better place to measure speed of a truck would be the front wheels since the axle load variations are smaller and no tractive torque affects it. Regardless of which wheel that is used for measuring speed its value is always affected by tire wear.

Distance [km]	5th wheel Without trailer	Dashboard Without trailer	Dashboard With trailer
Södertälje-Norrköping	121.8	122.8	123.5
Norrköping-Södertälje	122.8	123.7	124.5
Total	244.6	246.5	248.0

Table 7.5: Variations in measured distance with axle load.

7.2.2 Road Altitude

The sensitivity of the equipment for measuring road altitude was investigated by measuring the altitude of a fix point at different vehicle speeds and at different speeds of the fan in the cabin. The measurements are not conclusive but some observations are made. No connection between vehicle speed and measured altitude was found but when the fan in the cabin was increased from minimum to maximum the measured altitude dropped 15 m even though the vehicle stood still. The reason for this is that the equipment senses the air pressure within the cabin which was raised when the fan was increased. This change in measured level of altitude was repeated at other vehicle speeds which means that it is important to keep the fan in the cabin at constant speed.

The altitudes, measured with 3 Hz, are transformed to equally spaced points with 10 meters between points. The values from the test road in both directions are shown in Figure 7.4. As seen, the three different measurements are similar. However, in Figure 7.5 the standard deviation of the altitude measurements is shown for the return part of the test road. The values vary between 0-5 m over the distance. This means that the repeatability of the instrument not is as good as expected.

To find the accuracy of the instrument, reference values of altitudes along the road have been collected through official authorities responsible for roads and traffic in Sweden. Reference points where selected in the beginning, at the middle, and at the end of the test road. When passing these fix points like bridges, crossings etc a mark has been set in the log file of the instrument. A weakness with this approach is that marks are set "on the fly", meaning that it is hard to know if the references are precisely positioned. The measurements were adjusted to agree with the references in the beginning. In Figure 7.6 reference values at the middle of the test road are indicated with "+" and compared with mean values of the three altitude measurements. As seen the difference is about 2-3 m at both points. At all reference points the differences are between -2 - +3 m. This accuracy is good for a barometer but not as good as expected. In the future it would be interesting to compare these values with a GPS system.

7.2.3 Speed

During the road tests speed was measured only by the truck itself, presented to the driver though the dashboard and saved to files through the engine control
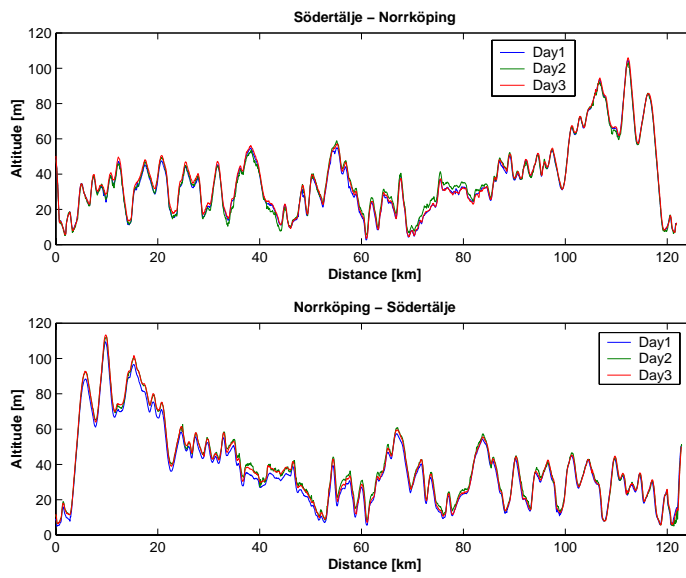
Figure 7.4: Measured topography of the test road.
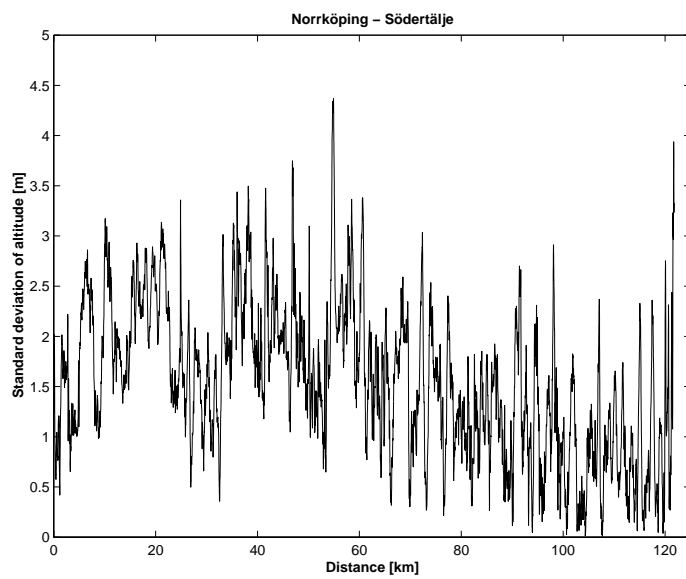
Figure 7.5: Standard deviation of the altitude measurements.
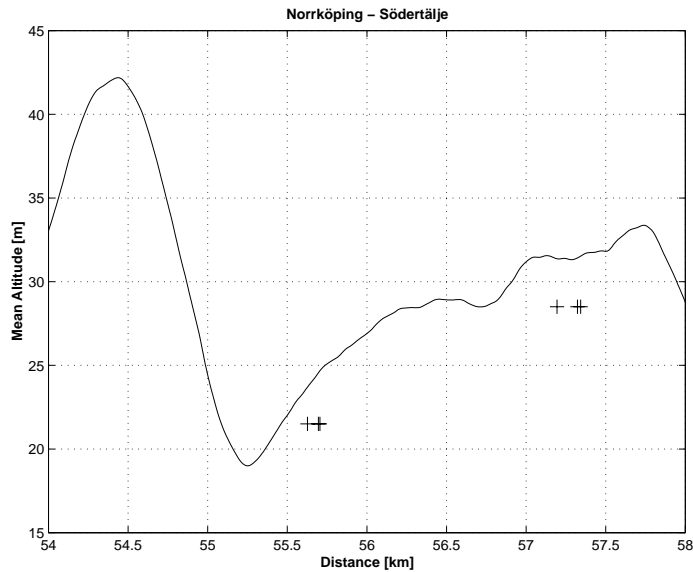
Figure 7.6: Mean measured altitudes compared with fix references.

unit and the instrument for the road profile. In Table 7.5 it is shown that the dashboard displayed too high values, a too long distance. The speed signal origins from the same source. Therefore the error in the speed signal is most likely constant over the speed range since it comes from the deflection of the tires on the drive axle. Assuming that the effective radius is constant at speeds over 30 km/h (as indicated in Section 3.4.1) and that the tractive force on the highway is small (slip is small) the recorded speed signal could be corrected using the quota from Table 7.5, 244.6/248.0. This means that the real speed was just below 84 km/h when the vehicle indicated 85 km/h. Slip is most likely the cause of this, since the offset is of the same magnitude as slip is expected to be. In Figure 7.7 the speed recorded on the test road at three different days are shown. The speed measurements show on a excellent agreement with small variations from time to time. The difference at 40 km from Norrköping is partly due to road construction work at the first test day.

The standard deviation of the measured velocity is shown in Figure 7.8. This is a measure of how good the test conditions were (free from disturbing traffic) and how equal the vehicle was driven from time to time. Beside from the road construction part, the deviations are largest in the beginning and in the end of the road. Some crossings and traffic interfered near the parking ground of the laboratory. Most part of the distance, on the highway, the deviations are only about 0.5 km/h. As explained before, the truck was on cruise control set at 85 km/h.
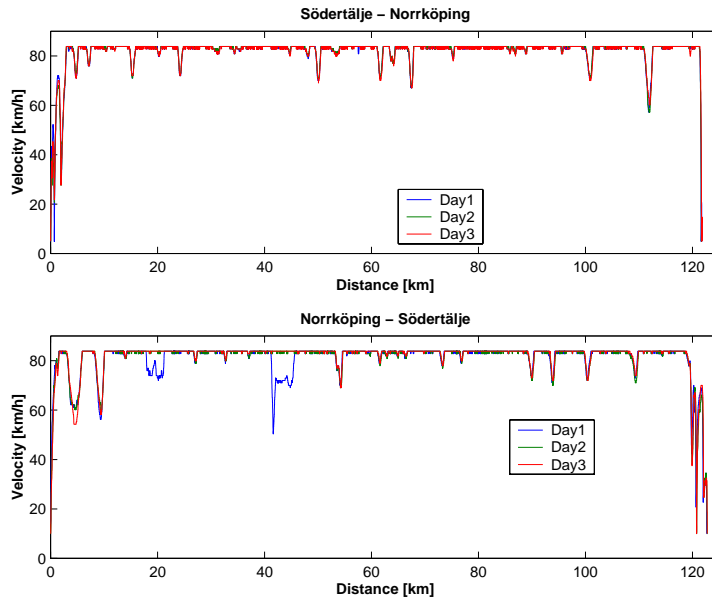
Figure 7.7: Measured speed of the test road.
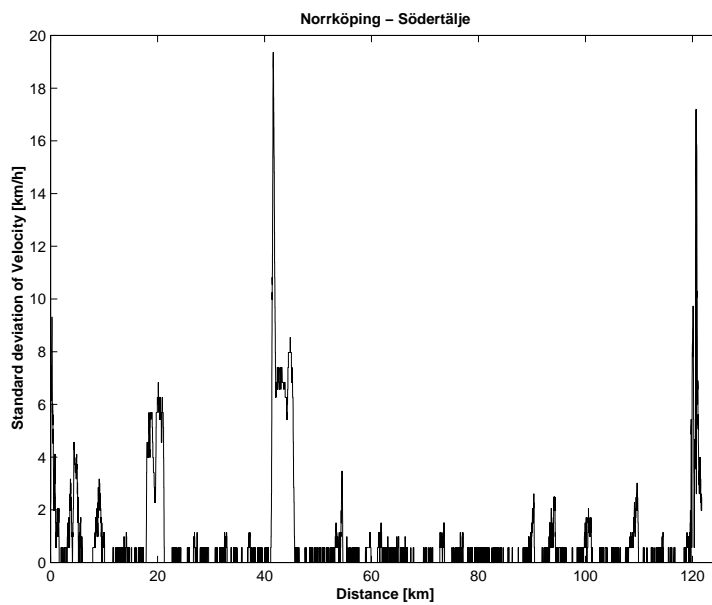
Figure 7.8: Standard deviation of measured velocity.

7.2.4 Engine

In Figure 7.9 the measured engine variables; engine speed, fueling and boost pressure are shown. The engine speed does not vary much in highway driving since it is rigidly connected to the vehicle speed. It is mainly centered around 1350 rpm. During gearshifts variations are shown. The cruise control, a PID controller, varies the fueling between 0 - 220 mg/stroke. The boost pressure follows the fueling with a slight delay like from a low pass filter.
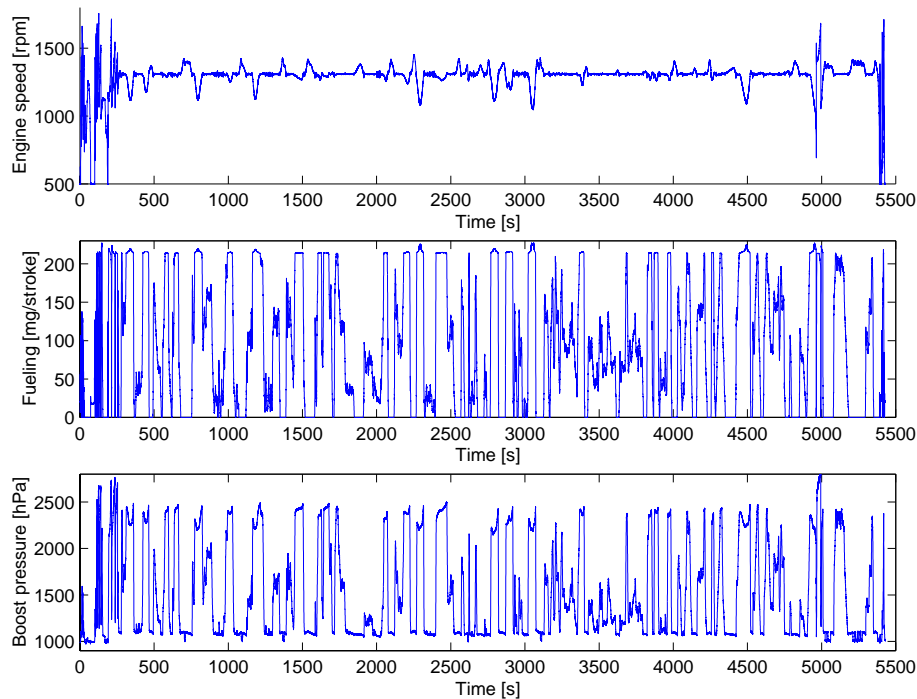
Figure 7.9: Engine variables during highway driving.

Boost Pressure

The purpose of the work presented in Chapter 5 was to ensure the correct load on the engine and thereby the correct fuel consumption. Since the engine model is described using values measured during steady state operation in engine test-cell it is also important to quantify how much of the operation that is in steady state for a heavy truck on the highway.

To quantify the operation of the engine during highway driving one solution is to study the boost pressure. Measured engine speed and fueling are used to calculate a corresponding steady state boost pressure, using steady state values

from engine test bed. This pressure is compared with measured values during operation. The difference between measured and calculated steady state boost pressure are shown in Figure 7.10. Important to remember is that the same engine was tested in test bed but another sensor for the boost pressure were used. The boost pressure build up is also limited by the smoke limiter in the control unit.
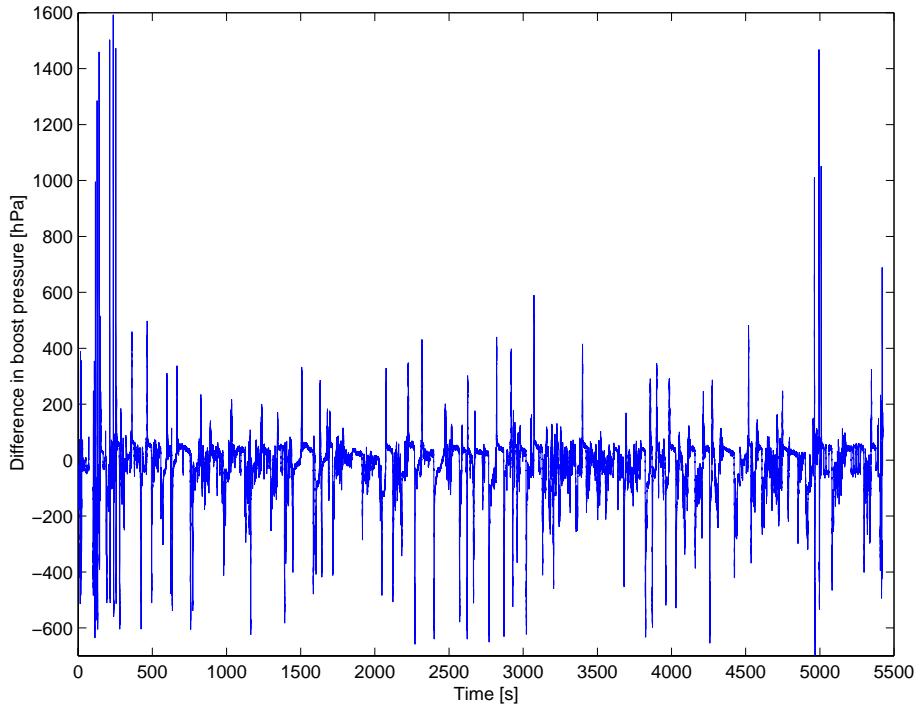
Figure 7.10: Difference between measured and calculated steady state boost pressure.

Some rather big differences in boost pressure are shown in Figure 7.10. Taking a closer look, as in Figure 7.11, it can be seen that these differences occur during gearshifts. Important to remember is that the model executes the gearshift instantly without time delay which can explain a part of the difference. The turbo can mathematically be seen as a low-pass filter and the differences seen here could be reduced by introducing a low-pass filter after the calculation of the steady state boost pressure. In normal operation the deviations are smaller, around 30 hPa.

It is concluded that a diesel engine in a heavy truck on the highway well can be described using steady state values from test cell. The boost pressure mainly deviates during gearshifts.
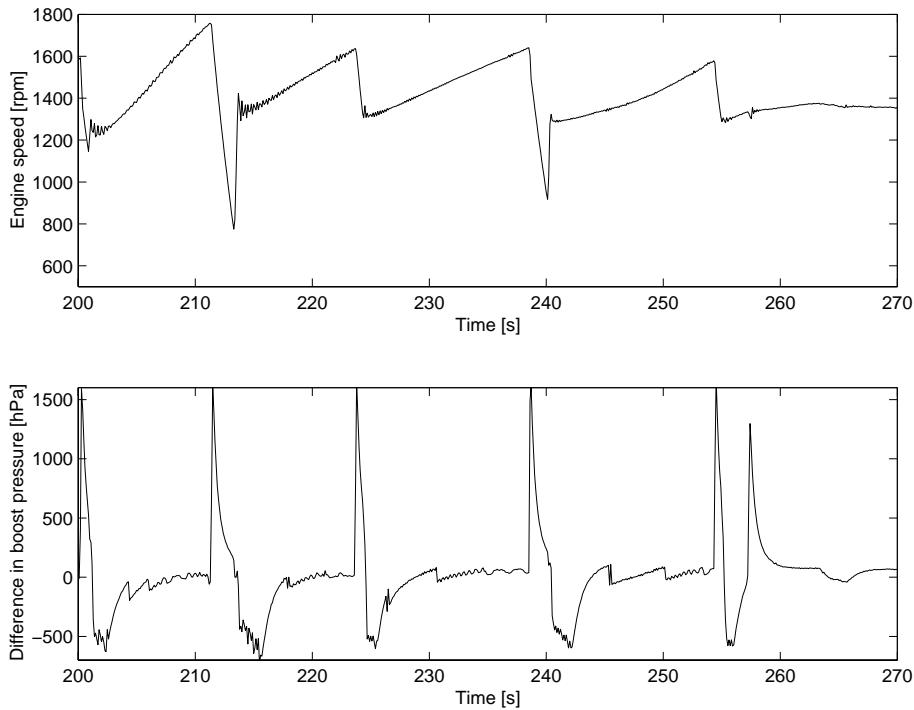
Figure 7.11: Difference in boost pressure during gearshifts.

Statistics

One way to statistically describe the operation of the engine is shown in Figure 7.12. It is a two dimensional map indicating how much time that is spend at each operational point (engine speed and load). As seen most of the time is spent between 1250 to 1400 rpm. Around 25% of the time is spent at engine drag (0% load). This is the time when no fuel goes into the engine, for instance when rolling down a hill or using the brakes. Almost the same amount of time, 20%, is spent at full load. The rest of the time is spent in other areas but mainly at part load between 1250 to 1400 rpm.

7.2.5 Fuel Consumption

In Table 7.6 the fuel consumption results for the three days are shown, values measured by the cans and the balance are compared with values from the control unit. It is seen that conditions during the test where good since it only differs 0.6 liters of fuel, using the cans, for the three tests. Both ways of measuring fuel show the highest fuel consumption on the second test. One possible explanation can be the change of driver on the second day. The third day the driver was
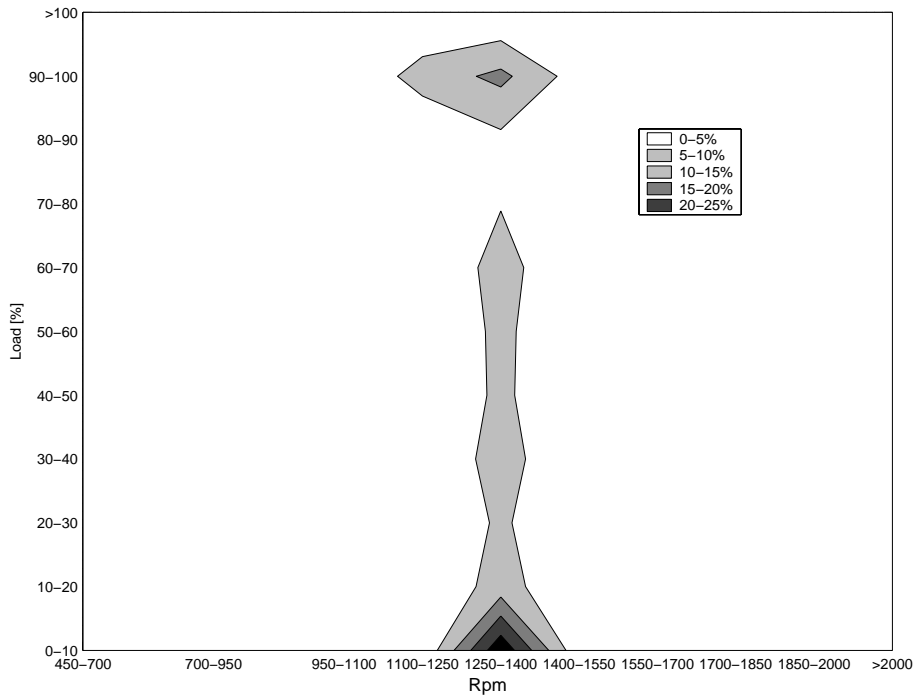
Figure 7.12: Distribution of operating time for the engine between Södertälje and Norrköping.

the same as on the second day. The control unit summarize to 3-4 liters of fuel more than if the cans and the balance are used. This means 4-5% too much and could depend on a difference between the amount of fuel commanded by the control unit and the amount that really is injected to the engine.

	Cans [L]	Control unit [L]
Day1	78.46	81.31 (+3.6%)
Day2	78.74	82.86 (+5.2%)
Day3	78.13	81.69 (+4.6%)

Table 7.6: Consumed fuel for a 40 ton truck on a test road.

7.3   Validation

In this section the previously presented results are compared with corresponding simulations and modifications are done to the model to achieve best agreement. Before the actual validation is started a sensitivity analysis is used to show how

variations in different parameters influence fuel consumption. The validation is done according to physical principles by studying continuously measurable variables like vehicle speed, engine speed etc.

7.3.1 Sensitivity Analysis

To study how sensitive the model is to changes in certain parameters a sensitivity analysis is conducted. Simulations are used where the most important parameters; vehicle mass m, frontal area A_f, coefficient of rolling resistance C_r, reference speed V_{ref} and *slope* of the road are varied 10% up and 10% down. The mean value of their impact on fuel consumption is shown in Table 7.7. The obtained differences in fuel consumption are scaled by the difference in parameter value ($\pm 10\%$) according to the following formula

$$\frac{\frac{f-f_0}{f_0}}{\frac{p-p_0}{p_0}} \tag{7.1}$$

where p_0 and f_0 are the nominal values of the parameter and the fuel consumption, p is the new parameter value and f is the new value of fuel consumption. This value can be used to study the impact on other changes than $\pm 10\%$.

Parameter $\pm 10\%$	Relative sensitivity on fuel consumption
m	0.53
A_f	0.36
C_r	0.29
V_{ref}	0.62
Slope	0.22

Table 7.7: The relative sensitivity on fuel consumption for some parameters.

The parameter with strongest influence is the reference speed. 10% higher reference speed gives 6.2% higher fuel consumption. This is not surprising since it influences the air resistance, the rolling resistance, and the engine speed (efficiency of the engine). A change in mass of 10% influence fuel consumption by 5.3%. This is the parameter with the second largest influence on fuel consumption and this is explained by the fact that the mass has a direct influence on the rolling resistance and on the resistance due to slope of the road. The frontal area influence only the air resistance and a 10% increase gives 3.6% higher fuel consumption. Noticeable is that a 10% change in air density influence just as much, as seen in Equation (3.5). The conclusion is that the influence from the weather is significant. During the three tests the air density varied $\pm 2\%$ according to Table 7.4 which influence fuel consumption by 0.7%. The two parameters with weakest influence on fuel consumption are the coefficient of rolling resistance and the slope of the road. The fact that the influence from the road is the

weakest is surprising but probably depends on that both positive and negative slopes are varied 10%.

This is not a true sensitivity analysis, since these changes influence the operational points of the engine and the result is dependent on how the efficiency of the engine vary in these points. Therefore these results are valid only for this particular vehicle model on this road. On another road or with another type of engine the result would be slightly different.

7.3.2 Speed

The recorded speed is used as input (reference speed) to the cruise control module in the simulations. If the measured speed was used directly this would cause some unwanted differences between the model and the real vehicle. For instance, the engine model would continue to produce power after passing the top of the hill since the reference speed increases. It would not start to break until the speed of the model has exceeded both the reference speed and the schwung limit (Section 3.5). This would give a difference in speed of 5 km/h. To avoid this, measured speeds above the reference speed of the real cruise control, 84 km/h, are replaced by 84 km/h.

The reference speed also shows some small fluctuations around 84 km/h originating from the real PID controller. There were also some parts where the real vehicle lost speed driving uphill. To give the cruise controller in the model a fix reference to work on and avoid using the output of the real cruise control as input for the controller in the model the reference speed of the road profile is changed and set to the constant value of 84 km/h. This corresponds to the constant reference speed set to the real cruise control during measurements.

These modifications led to a good agreement between measured and simulated speed. Remaining differences are in the simulations during the first/last part, driving to and from the highway.

7.3.3 Road Slope

Another important factor for good correlation between measured and simulated speed is inclination (slope) of the road. The altitude and position of the road was measured carefully and verified in the previous section. The simulation model though does not use the altitude, it uses the slope in every point to calculate resistance forces.

The slope is calculated by preprocessing the values measured on the road. At first a simple approximation of the derivative of the measured altitude was used. This gave too large variations and resulted in problems for the model to follow the reference speed. Uphill it lost speed faster than the real vehicle and downhill it gained speed faster. It seemed like the measurements needed to be filtered before calculating the slope for the model.

The *Fast Fourier Transform* is used to calculate a spectrum and to study its Bode diagram. Surprisingly it showed that the measured altitude almost only

contained very low frequencies. The explanation is that the measured data had already been smoothed. The test equipment was set to do a smoothing of the data by taking a weighted average of 5 points ahead and 5 points back. This procedure was repeated 5 times and resulted in some kind of low-pass filtering. In spite of this there was a need for more filtering.

Several low pass filters are tested on the measured altitude. To avoid offsets of the phase of the signal and delays these filters were implemented as zero-phase filters (the signal is filtered forward and reverse).

The evaluation of the filters is done in three steps.

1. A visual and subjective estimation of filtered altitude and calculated slope.

2. Comparing simulated and real speed in small downhills for different filters. Situations were chosen when no fuel was injected to the engine and no brakes were activated. If the altitude and the slope of the road has been calculated correctly the speed of the model at the bottom of the hill should agree with the speed of the real vehicle at this point since other forces were validated in Chapter 5.

3. Statistical methods like in Figure 7.12 are used to compare to total level of engine drag over the whole distance.

The visual estimation resulted in a Butterworth low-pass filter of 5th order with cut-off frequency 0.06. Since the sample frequency was 0.1 (values was recorded every 10th meter) this means that wavelengths below 166 m are removed.

When evaluating according to step 2 above, low-pass filters with other cut-off frequencies are tested as well. It was found to be hard to reach good agreement between simulated and measured speed in all three downhill slopes chosen on the road. Therefore stationary Kalman filters was tested as well. They were implemented as zero-phase filters according to the *Rauch-Tung-Striebel algorithm* (Gustafsson et al., 2001). The filters are based on a one-dimensional state space description with altitude as state variable. The covarians matrix Q is chosen to 1 and the covarians matrix R is chosen to 0.1 times the covarians of the measured altitude. For the comparison between simulated and measured speed in Figure 7.13 this filter has been used to calculate the altitude.

For the third step of the evaluation it was found that more filtering gave less operating time at engine drag. This is natural because eventually the road becomes flat and the engine can operate on constant load all the time. The real measurement had 25% of the time at engine drag. Before filtering the model showed around 33%. With this last filter the model spent about 30% of the time dragging as seen in Figure 7.14.

Important to remember is that the behavior in Figure 7.14 shows the fueling to the engine and is first of all dependent on the application of the cruise control. A poorly tuned controller would give the same result as fast variations of the slope of the road. In Figure 3.7 the behavior of the controller to a step in reference speed is shown. As seen the controller reacts fast and stable.
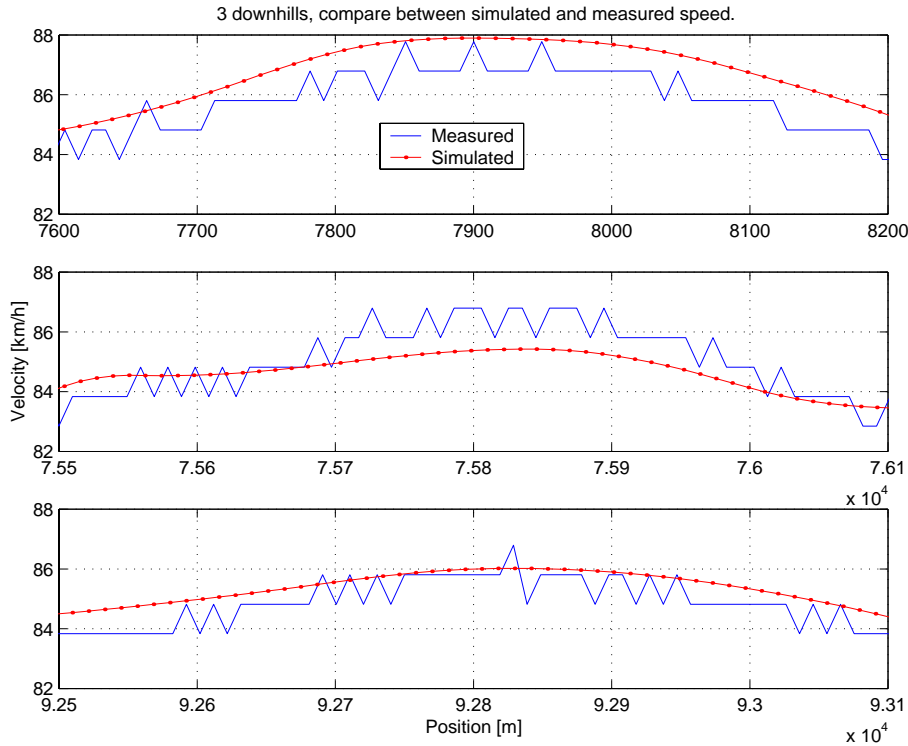
Figure 7.13: Comparsions between measured and simulated speed in three different down hill slopes. Several filters on the measured altitude were tested to reach good agreement.

It is concluded that the stationary Kalman filter described above for the measured altitude is most suitable. Thereafter the slope is calculated through a central difference approximation according to

$$ f'(x) = \frac{1}{12h}(-f(x+2h) + 8f(x+h) - 8f(x-h) + f(x-2h)) $$

where h is the step length.

7.3.4   Engine Speed

One important part in this validation is to check if the model has the correct engine speed since it together with fueling is used to calculate fuel consumption. By comparing engine speed in the model with the real engine speed at points where the vehicle speeds are the same it is concluded that all the ratios in the model (gearbox, final gear and wheel radius) are correct since no difference can be seen.

7.3.5 Engine Fueling

The hardest part to validate is the fueling to the engine. This is because fuel injection is the last part of the chain and is dependent on that all the parts in the powertrain have the right ratio and efficiency, that the rolling resistance and the tire radius are correct, that the air resistance is modeled correctly, that the weight of the vehicle is correct and that the reference speed and slope of the road are measured and calculated correctly. It gets even more complicated because in reality fueling is controlled by a PID controller, tuned with certain parameters and running with 20 Hz. In the model, fueling is controlled by another PID controller, tuned with other parameters and running with 5 Hz. Therefore it is very hard to achieve exactly the same output from the two controllers in every point.

One way to statistically verify the operation of the engine is shown in Figure 7.14. Compared to reality, shown in Figure 7.12, the model shows too much time at engine drag (1350 rpm, 0% load) and a few percent too little time at full load. This is found to be acceptable and probably depends on the slope of the road and the tuning of the controller as discussed before.
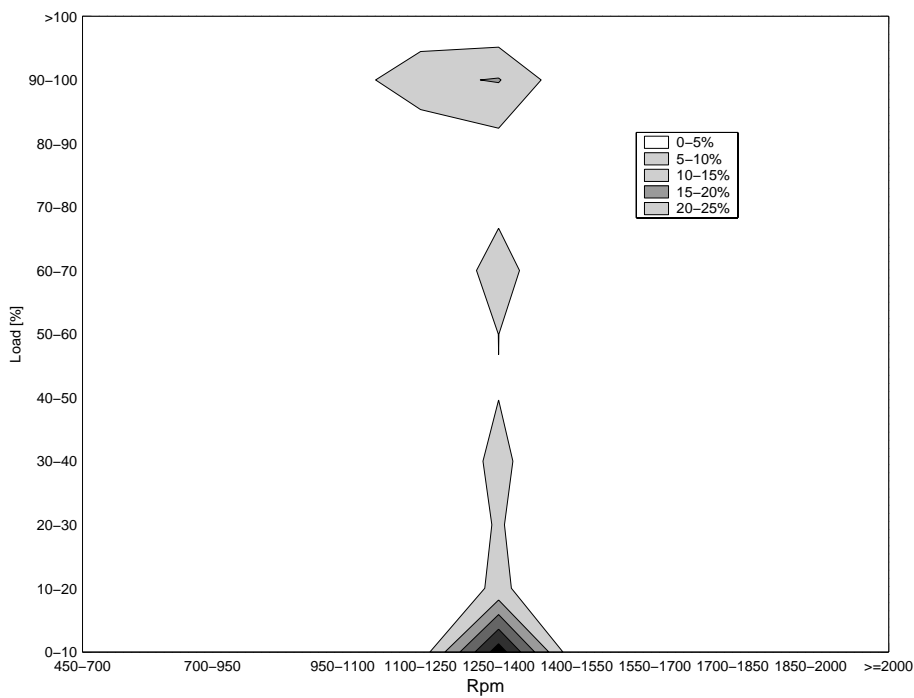
Figure 7.14: Distribution of operating time for the engine during the simulation between Södertälje and Norrköping.

7.3.6   Rolling Resistance

Before validating fuel consumption it must first be decided which model for
rolling resistance to use. Three different models are compared:

- Coefficient of rolling resistance dependent on tire temperature and vehicle
  speed, $C_r(T,v)$, as presented in Chapter 6.

- The optimized expression for $C_r(v)$, presented in Figure 5.7.

- Setting C_r to a constant value.

These three models have are used in simulations on the road from Södertälje to
Norrköping and back with conditions complying to the first test day. Table 7.8
shows fuel consumption results for these three rolling resistance models. As

Road	$C_r(T,v)$	$C_r(v)$	$C_r = constant$
Södertälje-Norrköping	37.99	37.53	37.50
Norrköping-Södertälje	38.73	38.62	38.60

Table 7.8: Comparsion of fuel consumption [L] for three different models for the
coefficient of rolling resistance.

expected the third model ($C_r = constant$) gives the lowest fuel consumption.
The first model ($C_r(T,v)$) is probably best but also the most complicated one.
It has two parameters more then the others, the time constant and initial tem-
perature. These results are obtained with a time constant of 0.5 h. It is also
important to estimate a good value of the temperature of the tire at the start of
the simulation. The ambient temperature is used as an approximation. During
the measurements there was a 15 minutes break in Norrköping in order to save
all measurements to files. During this break the tires were cooled of. This effect
is taken into account when setting the initial temperature of the tires when
simulating the trip back from Norrköping.

In the rest of this chapter the first model, described in Chapter 6, is used.

7.3.7   Fuel Consumption

The overall purpose with the simulations is to derive values of fuel consump-
tion. To compare simulations with measured values one must first decide which
reference for consumed fuel from Table 7.6 to use, cans or control unit . As dis-
cussed before, the most correct value of fuel consumption is derived using the
cans. But the cans were only used when the test road had been run forth and
back and after returning to the laboratory. So if trying to see if the difference
depends on the direction of the road the values from the control unit must be
used since the files from the control unit are saved after driving every direction
of the test road.

In Table 7.9 values of consumed fuel from the control unit are compared with the corresponding simulations. It is seen that the simulated values are about 2.5 liters less then the measured ones. The difference does not seem to depend on direction of the test road. The second test day does not fit in this pattern since it shows a small error on the first part and a large error on the second part of the test road. It is the measured values from this second part that differs largely from the other measurements.

	Road	Measured via control unit [L]	Simulated [L]
Day1	part1	39.97	37.99
	part2	41.34	38.73
Day2	part1	39.07	38.15
	part2	43.78	38.76
Day3	part1	40.48	38.37
	part2	41.21	39.05

Table 7.9: Real and simulated fuel consumption [L] for a 40 ton truck on the test road.

If instead, fuel consumption is compared over the whole distance then the cans can be used as reference. In Table 7.10 the simulated and measured (via cans) fuel consumptions are compared, in the unit liters/100km. As seen the simulated values are only 2% too low.

	Measured by cans	Simulated	Error
Day1	32.1	31.4	2.2%
Day2	32.2	31.4	2.3%
Day3	31.9	31.7	0.9%

Table 7.10: Comparsion of measured and simulated fuel consumption [liters/100km] for the whole test.

The fact that the simulations shows too low values of fuel consumption probably depends on the method for recording road data (measuring altitude with barometer and calculating slope) and on non modelled effects like:

- Higher rolling resistance on real roads due to rough surfaces and more cooling of the tires.

- Wind conditions at the test day, influence of side wind.

- Auxiliary units are used more in reality than in the model.

Anyhow, the results obtained are very good. The ability to simulate the whole truck driving on a road with an error of only 2 % from the real fuel consumption is better than all expectations.

7.4   Conclusions

In this chapter it is shown that reliable measurements of fuel consumption in real trucks are difficult to conduct. One of the hardest things to measure is the travelled distance because it depends on the rear axle load on the truck and slip. Due to the careful preparations a good repeatability could anyway be found in the fuel consumption measurements.

The instrument used to record altitude is not found to be good enough. It has a standard deviation of 0-5 m and an offset error of ± 3 m. Perhaps the largest weakness of this concept is that the slope of the road not is measured. Instead it is calculated as the difference from the measured altitude. In the future it would be interesting to try other methods of measuring road data, for example to use GPS to measure altitude or even better if the slope of the road could be measured directly.

For trucks in highway driving the boost pressure mainly deviates from steady state values during gearshifts and it is sufficient with an engine model based on steady state values.

It is also found that for fuel consumption predictions in highway driving the model produce a small error of 2%. This is a satisfying result.

8

Conclusions

In the competitive truck industry, one important sales argument is fuel consumption. To find more fuel efficient truck specifications a simulation program for predicting fuel consumption for trucks in highway driving has been developed. Its main purpose is to optimize the configuration of the powertrain for different transport tasks.

A longitudinal model of a truck is implemented in the modeling language Modelica. The model uses production code for speed and gear control, and uses exchangeable data sets to allow simulation of the whole production range of engine types, on recorded road profiles from all over the world. Combined with a graphical user interface this application is called STARS (Scania Truck And Road Simulation).

Two main types of experiments are conducted to validate the model. In the first type, the propeller shaft torque is measured on a heavy truck at different constant speeds. These measurements are used to validate the forces of air resistance and rolling resistance in the model. The major observation of this experiment is that rolling resistance for truck tires is strongly dependent on tire temperature and that the time constant for rolling resistance and tire temperature is long.

A new model for rolling resistance is developed that manage to describe the dynamic behavior of tires. The model relates rolling resistance to tire temperature and speed, and is used to explain and reproduce the experimental results.

To validate fuel consumption a test truck is driven on a highway and fuel consumption is measured. To be able to make comparing simulations the speed of the vehicle and the altitude of the road are recorded and processed. The

engine was prior to the test tested in an engine test-cell. It was shown that
for highway trucks it is sufficient with an engine model based on steady state
values. The boost pressure can be used as a transient indicator since it mainly
deviates from steady state values during gearshifts.

Due to the careful preparations a good repeatability is found in the fuel
consumption measurements. It is also found that for predictions of fuel con-
sumption in highway driving the model produce a small error of 2%, which is
a very satisfying result. The model can therefore under known conditions be
used to predict fuel consumption. Even under less known conditions the model
works fine for comparisons, for instance of powertrain configurations.

Bibliography

H. Bauer, editor. *Automotive Handbook Bosch*. Robert Bosch GmbH, 1996. ISBN 1-56091-918-3.

P. Bayle, J.F. Forissier, and S. Lafon. A new tyre model for vehicle dynamics simulations. *Automotive Technology International*, pages 193–198, 1993.

Paul N Blumberg. Powertrain simulation: A tool for the design and evaluation of engine control strategies in vehicles. *SAE*, SAE(760158), 1976.

Hilding Elmqvist, Dag Bruck, and Martin Otter. *Dymola User's Manual*, 1996.

Hilding Elmqvist and Sven-Erik Mattson. Modelica - the next generation modeling language an international design effort. World Congress on System Simulation (WCSS '97)., 1997.

Fredrik Gustafsson, Lennart Ljung, and Mille Millnert. *Signalbehandling*. Studentlitteratur, 2nd edition, 2001. ISBN 91-44-01709-X.

Nasser S. H., Weissermel V., and J. Wiek. Computer simulation of vehicle's performance and fuel consumption under steady and dynamic driving conditions. *SAE*, SAE(981089), 1998.

M. L. Janssen and G. L. Hall. Effect of ambient temperature on radial tire rolling resistance. *SAE*, SAE(800090), February 1980.

Uwe Kiencke and Lars Nielsen. *Automotive Control Systems*. Springer-Verlag, 2000. ISBN 3-540-66922-1.

Anders Kjell and Peter Asplund. Modellering och simulering av hydraulisk retarder. Master's thesis, KTH, Sweden, 1999. MMK 1999:4 MME657.

S. A. Lippman, K. L. Oblizajek, and J. J. Metters. Sources of rolling resistance in radial ply tires. *SAE*, SAE(780258), 1978.

H.B. Pacejka and E. Bakker. *The Magic Formula tyre model*, volume 21 of *Vehicle System Dynamics*. Proceedings 1st Tyre Colloquium, Delft, Oct. 1991, 1993.

Magnus Pettersson and Lars Nielsen. Driveline modeling and rqv control with active damping of vehicle shuffle. *SAE*, SAE(970536), 1997.

A. A. Popov, D. J. Cole, D. C. Cebon, and C. B. Winkler. *Energy loss in truck tyres and suspensions*, volume 33 of *Vehicle System Dynamics Supplement*, pages 516–527. Swets & Zeitlinger, 1999.

Johan Tengroth. Automatväxelsystem för lastbil. Master's thesis, Linköping University, SE-581 83 Linköping, 1999. LiTH-ISY-EX-2069.

H.C.A. van Eldik Thieme. *The Tire as a Vehicle Component*. S.K. Clark, Ed., Mechanics of Pneumatic Tires, Monograph 122 Washington DC National Bureau of Standards, 1971.

J. Y. Wong. *Theory of ground vehicles*. John Wiley & Sons, 2nd edition, 1993. ISBN 0-471-52496-4.